Chromosoma (2011) 120:481–499
DOI 10.1007/s00412-011-0327-8

RESEARCH ARTICLE

An intranucleolar body associated with rDNA

Saskia Hutten · Alan Prescott · John James · Stefanie Riesenberg · Séverine Boulon · Yun Wah Lam · Angus I. Lamond

Received: 2 February 2011 / Revised: 16 May 2011 / Accepted: 31 May 2011 / Published online: 23 June 2011

Abstract The nucleolus is the subnuclear organelle responsible for ribosome subunit biogenesis and can also act as a stress sensor. It forms around clusters of ribosomal DNA (rDNA) and is mainly organised in three subcompartments, i.e. fibrillar centre, dense fibrillar component and granular component. Here, we describe the localisation of 21 protein factors to an intranucleolar region different to these main subcompartments, called the intranucleolar body (INB). These factors include proteins involved in DNA maintenance, protein turnover, RNA metabolism, chromatin organisation and the post-translational modifiers SUMO1 and SUMO2/3. Increase in the size and number of INBs is promoted by specific types of DNA damage and depends on the functional integrity of the nucleolus. INBs are abundant in nucleoli of unstressed cells during S phase and localise in close proximity to rDNA with heterochromatic features. The data suggest the INB is linked with regulation of rDNA transcription and/or maintenance of rDNA.

Introduction

The interphase nucleus of a eukaryotic cell is highly compartmentalised. It contains subnuclear domains such as the nucleolus, splicing speckles, paraspeckles, Cajal and PML bodies, with the nucleolus being the most prominent subnuclear compartment (Handwerger and Gall 2006; Austin and Bellini 2010; Boisvert et al. 2007). The nucleolus has a primary role in ribosome subunit biogenesis, with additional functions including acting as a stress sensor and in cell cycle control, leading to the view of the nucleolus as being multifunctional (Boisvert et al. 2007; Boulon et al. 2010; Pederson 1998; Pederson and Tsai 2009). Like other

Communicated by E. Nigg

Electronic supplementary material The online version of this article (doi:10.1007/s00412-011-0327-8) contains supplementary material, which is available to authorized users.

S. Hutten · S. Riesenberg · S. Boulon · A. I. Lamond (✉)
Wellcome Trust Centre for Gene Regulation and Expression,
College of Life Sciences, University of Dundee,
Dundee DD15EH, UK
e-mail: angus@lifesci.dundee.ac.uk

A. Prescott
Division of Cell Biology and Immunology,
College of Life Sciences, University of Dundee,
Dundee DD1 5EH, UK

J. James
Microscopy Facility, College of Life Sciences,
University of Dundee,
Dundee DD1 5EH, UK

Y. W. Lam
Department of Biology and Chemistry,
City University of Hong Kong,
Kowloon, Hong Kong

Present Address:
S. Riesenberg
Life and Medical Sciences Bonn (LIMES),
Genomics and Immunoregulation, University of Bonn,
53115 Bonn, Germany

Present Address:
S. Boulon
CNRS-CRBM, Université Montpellier 2,
34293 Montpellier, France

nuclear domains, the nucleolus is a dynamic compartment, and both its protein composition and general architecture change in response to environmental conditions (Andersen et al. 2005; Boisvert et al. 2010; Shav-Tal et al. 2005). In addition, many nucleolar proteins are not exclusive to the nucleolus and also localise to other subcellular domains.

The nucleolus forms around arrays of ribosomal DNA (rDNA) on the five acrocentric chromosomes (chromosomes 13, 14, 15, 21 and 22 in human), the so-called nucleolar organizer regions (NORs). Human NORs consist of clusters of ~400 individual rDNA repeats in total (per diploid genome); however, only a subset of these is transcribed. Active rDNA is distinguishable from inactive rDNA by specific epigenetic marks (i.e. DNA methylation and histone modification status) as well as by associated proteins. Inactive rDNA carries heterochromatic features, such as hypermethylated CpG islands at the rDNA promoter or hypermethylated histones like H3K9, with the latter leading to the association of heterochromatin protein 1 (HP1; reviewed in Huang et al. (2006) and McStay and Grummt (2008)). Active rDNA, in contrast, is enriched in acetylated histones H3 and H4, and its promoter is hypomethylated. Additionally, factors of the RNA polymerase I (RNA pol I) machinery, including the upstream binding factor (UBF), are associated with the entire rDNA repeat and keep it in an undercondensed state (reviewed in Sanij and Hannan (2009)). In the current model, regulation of rRNA transcription occurs by either changing the transcription rate of already active rDNA repeats and/or the number of transcriptionally active repeats. This can vary depending on the cell type, or during differentiation and development (Haaf et al. 1991). The mammalian nucleolar remodelling complex is responsible for the coordination of factors regulating heterochromatin formation on rDNA (Santoro and Grummt 2005; Santoro et al. 2002; Strohner et al. 2001; Zhou et al. 2002). Interestingly, maintenance of heterochromatic rDNA by DNA repair mechanisms has recently also been linked to nucleolar and rDNA repeat integrity and may even influence heterochromatin formation elsewhere in the nucleus (Paredes and Maggert 2009; Peng and Karpen 2007), suggesting more extensive roles for nucleolar chromatin organisation.

In higher eukaryotes, the tripartite nucleolar architecture reflects the three main steps in ribosome subunit biogenesis, i.e. rDNA transcription, rRNA processing and ribosome subunit assembly. The fibrillar centre (FC) is enriched in components of the RNA pol I machinery. Transcription of rRNA is believed to take place either in the FC or at the border between the FC and the surrounding dense fibrillar component (DFC). The DFC is enriched in rRNA-processing factors, including snoRNAs and the snoRNP proteins such as fibrillarin and Nop58. Both the FC and DFC are embedded in the granular compartment (GC), where pre-ribosome subunits are assembled (reviewed in Boisvert et al. (2007) and Sirri et al. (2008)). However, a number of publications have described factors localising to nucleolar regions different from FC, DFC or GC, probably revealing the existence of additional subnucleolar regions. First, coilin, Sm proteins and splicing snRNPs were detected within the nucleolus of specialized cell types in hibernating dormice, and in human breast cancer or HeLa cell lines upon phosphatase inhibition (Lyon et al. 1997; Malatesta et al. 1994; Ochs et al. 1994). More recently, SUMO1 and the nuclear transport factor CRM1 were found in discrete intranucleolar foci (Desterro et al. 2005; Ernoult-Lange et al. 2009). However, the mechanisms causing this intranucleolar localisation have so far not been characterized in detail.

In this study, we identify proteins associated with RNA metabolism, protein turnover and DNA maintenance that localise to a distinct subnucleolar region separate from the FC, DFC and GC. We show the same intranucleolar structure, termed intranucleolar body (INB), can also be found in animal tissue and demonstrate it is promoted by specific DNA-damaging conditions without disrupting the structural and functional integrity of the nucleolus.

Materials and methods

Cell culture and transfections

HeLa, HEK293, C33A, HaCaT, HCT116, HepG2, HT1080, MCF7, U138 and U2OS cells were grown in DMEM (Invitrogen) containing 4.5 g/l glucose, 10% FCS, 2 mM glutamine, 100 U/ml penicillin and 100 μg/ml streptomycin. Tera-1 cells were grown in McCoy's 5a medium (Invitrogen) containing 20% FCS, 2 mM glutamine, 100 U/ml penicillin and 100 μg/ml streptomycin. CHO cells were grown in MEM α medium (Invitrogen) in the presence of 10% FCS, 2 mM glutamine, 100 U/ml penicillin and 100 μg/ml streptomycin. The stable HeLa cell line for EYFP-SUMO1 was generated and maintained by standard protocols using 400 μg/ml G418 as selective marker (Trinkle-Mulcahy et al. 2007). HeLa cells stably expressing His-SUMO1 were a gift from Ron Hay (University of Dundee) and were maintained using 1 μg/ml puromycin. Transient transfections were performed with Effectene (Qiagen) according to the instructions of the manufacturer.

Bovine lens and human skin processing

Bovine eyes were obtained fresh from the abbatoir and the lens dissected from the posterior aspect of the eye. Human skin samples were collected from patients undergoing

surgery to revise scars at Ninewells Hospital, Dundee. Full ethical permission was obtained for the use of these tissue samples for research purposes. The skin samples were trimmed to a suitable size for sectioning; excess fat was removed. The tissues were frozen in iso-pentane cooled in liquid nitrogen and stored at −80°C prior to sectioning. Samples were sectioned at 20 μm on a Leica CM3050S cryostat.

Stress and drug treatment

To introduce DNA double strand breaks (DSBs) by gamma irradiation (IR), cells were exposed to 10 Gy using a ^{137}Cs source and left to recover for the times indicated. Alternatively, cells were incubated for 24 h in the presence of either 2 mM hydroxyurea (HU; Sigma), 25 nM camptothecin (CPT; gift from John Rouse (University of Dundee)) or for 3 h in the presence of 50 μM etoposide (eto; Sigma). UV-C irradiation was performed as described in Cioce et al. (2006) and cells left to recover for 3 h. 4-Nitroquinoline 1-oxide (NQO, Sigma) was used as UV-mimetic agent at 1 μM for 3 h. To specifically inhibit RNA polymerase I transcription, cells were incubated in the presence of 5 nM actinomycin D (actD; Sigma) for times as indicated.

Plasmids

The cDNA for PA28γ and PPM1G was inserted into pEGFP-C1 (clontech) via BamHI and HindIII or BglII and KpnI, respectively. pcDNA-mCherry was generated by insertion of mCherry via Asp718 and BamHI into pcDNA4 (Invitrogen; gift from Archa Fox (Western Australia Institute for Medical Research)). The cDNA for fibrillarin was inserted into pcDNA4-mCherry via BamH1 and EcoRI. The cDNA for SENP3 and SENP5 was cloned into pmCherry-C1 XhoI and SalI or HindIII and SalI, respectively. pDendra2-C1 was generated by replacing the ORF for GFP by Dendra2 in the pEGFP-C1 backbone using PCR without affecting the MCS, and the cDNA for SUMO1 inserted via BglII and SalI to obtain Dendra2-SUMO1. The 11.9-kbp EcoRI rDNA probe was a gift from Brian McStay (NUI Galway, Ireland). GFP-SUMO1 and GFP-SUMO2/3 were gifts from Ron Hay (University of Dundee).

Antibodies

Antibodies were used as follows for immunofluorescence studies: mouse anti-RPA194 (Santa Cruz; 1:50), anti-fibrillarin (monolayers: abcam; 1:300; lens tissue sections: 72B9, Cytoskeleton Inc., 1:10), anti-B23 (Sigma; 1:500), anti-CDC5L (BD; 1:200), anti-TRIM28 (BD; 1:300), anti-DPK (Calbiochem; 1:100), anti-Ku70 (abcam; 1:100), anti-PA28γ (BD; 1:100), anti-TMG (Oncogene; 1:10), anti-coilin (5P10; 1:10 (Rebelo et al. 1996)), anti-HP1α (euromedex; 1:500) and anti-CPD (CosmoBio Co, LTD.; 1:1,000); and anti-RNA polymerase II CTD repeat (4H8, abcam; 1:300); rabbit anti-PPM1G (Bethyl laboratories; 1:300), (mouse) anti-RNA polymerase II CTD repeat (4H8, abcam; 1:300) anti-nucleolin (abcam; 1:1,000), anti-PA28γ (MBP; 1:300), anti-UBF (HPA/Sigma; 1:100), anti-H3K9me3 (abcam; 1:100), anti-H4K16ac (milipore upstate; 1:100), anti-H4K20me3 (abcam; 1:400), anti-phosphoSer139 H2AX (upstate; 1:200) and anti-PCNA (abcam; 1:300); goat anti-Nop58 (Santa Cruz; 1:100); and sheep anti-SUMO1 and SUMO2/3 (gift from Ron Hay (University of Dundee); 1:300 or 1:100 for monolayers respectively, 1:20 for EM and tissue sections). For western blot, the rabbit anti-phosphoSer139 H2AX antibody was used 1:500 in 3% milk in TBS/0.1% Tween.

Immunofluorescence and fluorescence microscopy

For immunofluorescence staining of cell monolayers, HeLa cells were grown on poly-L-lysine-coated coverslips, fixed in 3.7% paraformaldehyde/PHEM buffer (120 mM PIPES, 55 mM HEPES, 20 mM EGTA, 8 mM MgSO4, pH 7) for 7 min and permeabilized in 1% TX-100/PBS for 15 min at room temperature (RT). Cells were blocked for 10–15 min in blocking buffer (0.2% fish gelatine [Sigma] in PBS) and incubated with primary antibodies in blocking buffer for 1–2 h at RT. Secondary antibodies were from Molecular Probes (donkey anti-mouse or rabbit Alexa 488, Alexa 594 or Alexa 647, anti-goat Alexa 488 or anti-sheep Alexa 488 or Alexa 546). Washing steps were performed with PBS/0.1% Tween-20. DNA was stained with Hoechst at 12.5 μg/ml in PBS and cells mounted in Vectashield (Vector Laboratories, Burlingame, CA, USA). Images were acquired with a DeltaVision Core Restoration microscope mounted on an Olympus IX71 stand with a ×60 1.42 NA oil immersion objective lens using either 1×1 or 2×2 bin with a section spacing of 0.2 μm. Exposure time was set to provide an intensity of ~1,000 counts on a 12-bit Coolsnap HQ camera (Roper, USA). Processing and analysis was performed using SoftWorx (Applied Precision) and Adobe Photoshop. To determine the diameter of the INB in HeLa and U2OS cells, the area of the INB was measured at its largest dimension in *z* in 10–20 cells using the polygon function in SoftWorx. The diameter was then calculated under the premise of a circular shape of the INB from the obtained values.

For immunofluorescence of lens and skin tissue sections, frozen sections were fixed in 4% paraformaldehyde in PBS, permeabilised with 1% Nonidet P40 in PBS, blocked with normal donkey serum (10%), stained with sheep anti-SUMO2 and mouse anti-fibrillarin and counterstained with donkey anti-sheep IgG Alexa 488, donkey anti-mouse IgG Alexa 594 and DAPI. Sections were imaged on an LSM700

laser scanning confocal microscope (Carl Zeiss) using a ×100 alpha Plan-Apochromat objective (NA 1.46).

Time-lapse imaging, FRAP and photoconversion

All live cell experiments were performed ~18–24 h after transient transfection using a DeltaVision Spectris wide field deconvolution microscope/Olympus IX71 stand in a 37°C chamber with CO_2-independent medium. For time-lapse microscopy and fluorescence recovery after photobleaching (FRAP) analysis, images were acquired using an Olympus ×60 1.40 NA oil immersion objective lens and either 2×2 bin or 4×4 bin, respectively. FRAP and Photoconversion experiments were done using a DeltaVision Core Restoration Microscope equipped with a Quantifiable Laser Module (Applied Precision). For FRAP, imaging and bleaching conditions were chosen to match proteins with the highest turnover by using a 4×4 bin. A 488-nm diode laser was used to bleach to approximately 50% of initial intensity. For photoconversion, intranucleolar Dendra2-SUMO1 was photoconverted using the 405-nm laser at low intensity (10%) to avoid photodamage. Images were acquired using an Olympus ×100/1.35 NA lens and 4×4 bin using low exposure times in order to avoid further photoconversion due to light exposure during image acquisition.

Preparation of nucleoli

Nucleoli were isolated from HeLa cells (ten 14-cm dishes) as previously described (Andersen et al. 2005) except that a 0.35 M sucrose buffer supplemented with 2.5 mM $MgCl_2$ was used. The final nucleolar pellet was resuspended in 0.35 M sucrose/0.5 mM $MgCl_2$, frozen in liquid N_2 and stored at −80°C.

Electron microscopy

Isolated nucleoli and whole cells were fixed in 4% paraformaldehyde in 0.2 M PIPES, washed, cryoprotected in 2.3 M sucrose and frozen in liquid nitrogen. Semi-thin sections (200 nm for scanning electron microscopy (SEM)) and ultra-thin sections (70 nm for transmission electron microscopy (TEM)) were cut on a Leica Ultracut EM-FCS cryo-ultramicrotome. Semi-thin sections were collected on polished silicon wafer (Agar), post-fixed with 1% gluteraldehyde and 1% OsO_4 in PBS, critical point dried and sputter coated with gold/palladium. The semi-thin sections were imaged at high vacuum on an XL-30 ESEM (FEI). Ultra-thin sections were collected on Formvar/carbon-coated grids and immunolabelled with SUMO1 antibody followed by rabbit anti-sheep IgG and Protein A colloidal gold (BBI). The immunogold-labelled sections were imaged on a Tecnai 12 TEM (FEI).

DNA FISH

For combined immunofluorescence and rDNA FISH, cells were grown on microscope slides, and the immunofluorescence was performed as described above except that the primary and secondary antibody were used two to five times as concentrated, respectively. After washing of the secondary antibody, cells were fixed again for 10 min in 3.7% PFA/PHEM and gradually warmed up to 75°C in a water bath for 45 min in 2× SSC. Cells were incubated 10 min each in 70% ethanol and absolute ethanol, and DNA was subsequently denatured by 10 min incubation in 0.1 M NaOH. Cells were incubated 7 min in 2× SSC and finally dehydrated by 10 min incubation in 70% ethanol followed by 10 min in absolute ethanol. Slides were air-dried and pre-warmed for 5 min at 37°C before the hybridization.

FISH-probe Five microgrammes of plasmid coding for the 11.9-kb EcoRI restriction fragment corresponding to the human intergenic spacer sequence (IGS) upstream of the gene promoter for rDNA (Mais et al. 2005) was nick-labelled with 1 mM Cy3-dCTP or Cy5-dCTP using a nick-translation kit (GE Healthcare Life Sciences) according to the manufacturer's instructions. One microgramme of labelled probe was precipitated in ethanol and 0.3 M sodium acetate together with 10 μg COT1 carrier DNA (Invitrogen) and dissolved in 12 μl hybridization buffer (Hybrisol, Abbot Molecular, Maidenhead, UK). A directly labelled fluorescent telomeric probe for the short arm of chromosome 4 (4p) was obtained from Cytocell (Cambridge, UK). Probes were pre-warmed at 37°C for 5 min.

Hybridization and washing Probes were added to pre-warmed slides, and slides were sealed with a coverslip and rubber cement, subsequently denatured for 2 min at 75°C and hybridized in a wet chamber overnight at 37°C. After removing the coverslips, slides were washed in 2× SSC at 75°C for 2 min, 1 min in 0.4 SSC/0.05% TX-100 at RT and rinsed briefly in PBS. DNA was counterstained with Hoechst as described above.

Metabolic labelling of rRNA with 5-ethynyl uridine (EU) or [5,6-^{3}H]uridine

Labelling of RNA by 5-ethynyl uridine (EU) for microscopy was performed using the Click-IT RNA Imaging kit (Invitrogen) according to the manufacturer's instructions. Labelling of newly synthesized rRNA with [5,6-^{3}H]-uridine

was performed according to Pestov et al. (2008). Total RNA was isolated (Qiagen RNA kit), and equal amounts of total RNA were loaded onto an agarose gel, electroblotted onto a nylon membrane and analysed by autoradiography.

Counterflow centrifugal elutriation (CCE) and cell cycle analysis by flow cytometry

To enrich for cells in G1 phase, counterflow centrifugal elutriation (CCE) was performed with ~1.5–2.0×10^8 of exponentially growing HeLa cells according to Kaufman et al. (1990) using a Beckman J6-MI centrifuge and a JE-6B elutriation rotor at 3,000 rpm at room temperature. The G1-fraction was washed once in DMEM and cells re-seeded for cell cycle progression into dishes with coverslips.

For analysis of the cell cycle stage, cells were trypsinized at different time points after re-seeding (2, 12 and 18 h), washed in PBS/1% BSA and fixed in ice-cold 70% ethanol for at least 30 min at room temperature or overnight. DNA was stained using 50 μg/ml propidium iodide in the presence of 50 μg/ml RNase-A and 0.1% TX-100. Data were acquired using a FACS Calibur cytometer (Becton Dickinson, USA) and CellQuest software. Cells were gated by their forward and side scatter profiles, and cell cycle analysis was performed using the Watson (pragmatic) model in the FloJo software (Treestar, USA).

Results

The intranucleolar body is a distinct nucleolar compartment

We and others have observed protein components including coilin, the splicing factor CDC5L and the post-translational peptide modifier SUMO1 in a discrete region within the nucleolus (Ajuh et al. 2001; Desterro et al. 2005; Lyon et al. 1997; Malatesta et al. 1994; Ochs et al. 1994; Sleeman et al. 1998; Sleeman and Lamond 1999). Here, we show that PA28γ/PSME3, the nuclear isoform of the 11S proteasome activator complex, displays a similar localisation in the nucleolus. PA28γ has been shown to interact with the 20S proteasome in an ubiquitin-independent degradation pathway for cellular proteins including p21, p16 and p19 (Chen et al. 2007). Previously, we have demonstrated that PA28γ is a mediator in the response of Cajal bodies to UV-C stress (Cioce et al. 2006). The intranucleolar location for PA28γ does not overlap with any of the markers for the three main nucleolar compartments, as shown by co-immunofluorescence with either the RNA polymerase I subunit RPA194 as a marker for the FC, fibrillarin for the DFC or B23 for the GC (Fig. 1a, arrows). PA28γ forms a discrete spot in the same region within the nucleolus as both coilin and CDC5L (arrows in Fig. 1b and data not shown), suggesting they localize to the same subnucleolar structure. In accordance with earlier publications, we also found SUMO1 to form distinct intranucleolar spots in HeLa cells stably expressing YFP-SUMO1, similar to the localisation of PA28γ (Desterro et al. 2005 and Fig. 1b, arrows). We also found endogenous SUMO1 forming intranucleolar bodies (INBs), however with reduced size and abundance as compared with cells stably expressing YFP-SUMO1 or His-SUMO1 (data not shown). We conclude the INB localisation is not only caused by overexpression of SUMO1. The SUMO localisation likely corresponds to SUMO1 conjugated to substrate proteins because a non-conjugatable SUMO1 mutant missing the last two amino acids (SUMO1ΔGG) does not form an INB (Desterro et al. 2005; data not shown). Also, overexpression of the nucleolar forms of SUMO-specific proteases SENP3 or SENP5, but not of the nucleolar marker fibrillarin, led to a loss of the INB staining for YFP-SUMO1 (Fig. 1c).

In addition to PA28γ and SUMO1, we have identified 19 protein factors that localise to the same INB structures using validated antibodies against commonly used nuclear markers (as shown in Table 1). This includes proteins involved in DNA repair and replication, protein turnover, RNA processing and chromatin organisation as well as SUMO2/3. An antibody against the 5′-terminal trimethyl-guanosine cap structure (TMG) also labels the same INB, suggesting the presence of small RNAs such as snRNA or snoRNAs (Fig. 1b). This is in agreement with earlier findings that reported the presence of several U snRNPs within the mammalian nucleolus (Ganot et al. 1999; Gerbi and Lange 2002; Lyon et al. 1997; Sleeman et al. 1998; Sleeman and Lamond 1999; Tycowski et al. 1998) as well as the presence of TMG-labelling in the yeast nucleolus (Potashkin et al. 1990).

The INB appears totally enclosed within the nucleolus, as judged by fibrillarin or nucleolin co-staining, and therefore is not likely to be a nucleoplasmic invagination. Other nuclear proteins, such as RNA polymerase II, the SR protein SRp55 and topoisomerase II beta (Fig. 1b and data not shown), are not detected within the INB, suggesting only specific factors localise to this sub-region within the nucleolus. For some factors, we observe a partial overlap within the INB (e.g. coilin and PA28γ (Fig. 1b)). The INB detected with YFP-SUMO1 appears surrounded by an outer shell of PA28γ (Fig. 1b). This suggests that these proteins each occupy a defined space or associate differentially with structures within the INB, rather than localise there by diffusion, as had been suggested for p53 (Kruger and Scheer 2010).

The INB can be found in ~30–40% of HeLa cells and also in other cells types, albeit with different frequencies (see Table 2). The INB exists mostly as a single nucleolar body; however, multiple INBs per single nucleolus can

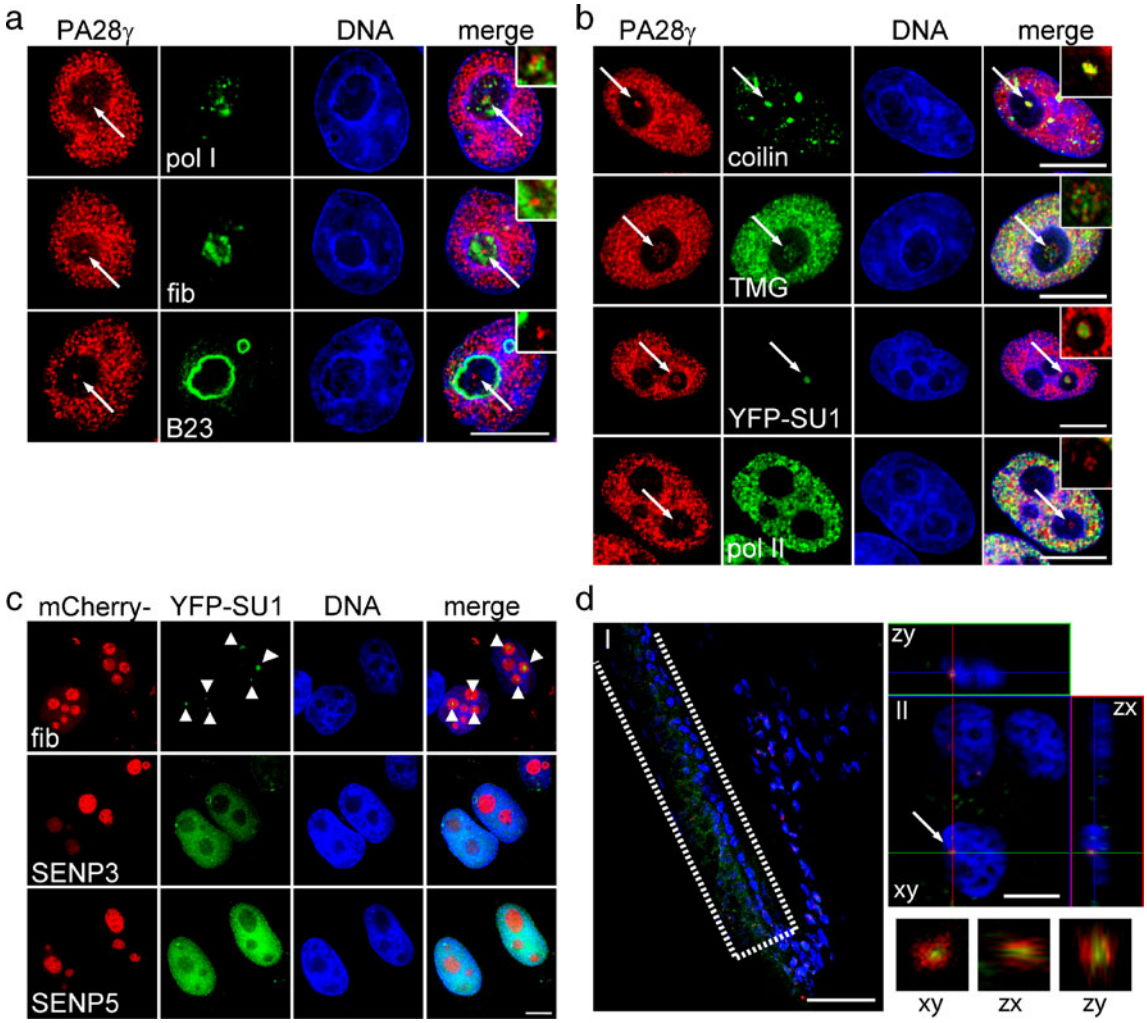

Fig. 1 The intranucleolar body is a sub-nucleolar compartment distinct from known nucleolar regions. **a** HeLa cells were stained by specific antibodies for PA28γ and either the RPA194 subunit of the RNA pol I complex (pol I), fibrillarin (fib) or B23 as marker proteins for the FC, DFC or GC, respectively. The INB is indicated by *arrows*. *Bar*, 10 μm. **b** HeLa cells were double labelled with specific antibodies for endogenous PA28γ and either coilin, the 5′-terminal trimethylguanosine cap structure (TMG) or the C-terminal domain of RNA pol II (pol II). In the *third row*, HeLa cells stably expressing EYFP-SUMO1 were used to stain for endogenous PA28γ. The INB is indicated by *arrows*. *Bar*, 10 μm. Note that no DNA stain is shown in the *insets*. **c** HeLa cells stably expressing EYFP-SUMO1 were transiently transfected with constructs coding for either mCherry-fibrillarin (fib), -SENP3 or -SENP5 and analysed for the presence of the intranucleolar SUMO1-body (*arrowheads*) by fluorescence microscopy. Note that for reasons of visibility, different exposure times were used for YFP-SUMO1. *Bar*, 10 μm. **d** Bovine lens tissue sections were processed and stained with specific antibodies to SUMO2 (*green*) and fibrillarin (*red*) and subsequently analysed by confocal microscopy. A cross section through the whole lens is shown in (*I*) with the epithelial layer indicated by a *box*. *Bar*, 50 μm. A midplane of epithelial cells in all three planes is shown in (*II*). The INB is indicated by an *arrow*. *Bar*, 5 μm. Magnifications of a nucleolus with SUMO2-intranucleolar body in all three midplanes are enlarged in the *panel below*. For clarity, only the stain for SUMO2 (*green*) and fibrillarin (*red*) is shown here

occasionally be observed. The diameter of an INB can vary from ~0.5 to 1.6 μm in HeLa and ~0.4 to 1.0 μm in U2OS cells.

To investigate whether the INB results from cell transformation and/or culturing conditions, we analysed primary cells from animal tissue for the presence of the INB. The eye lens offers the opportunity to analyse cells of different developmental stages and with different levels of transcriptional activity in a single histological section (Dahm et al. 1998; Gribbon et al. 2002). Examining cross sections of bovine lens, we found that antibodies against SUMO2 stain a discrete spot within the nucleolus of the epithelial layer (Fig. 1d). This SUMO2 signal is completely surrounded by fibrillarin as shown by the projections in all three planes and therefore likely to correspond to the same INB observed before in cultured cell lines (arrow in Fig. 1d panel II and magnification thereof). This intranucleolar localisation can be spatially distinguished from nucleoplasmic foci, presumably PML bodies, found adjacent to the nucleolus. Using specific antibodies, no PML could be

Table 1 Components identified within the intranucleolar body (INB)

Protein names	Uniprot	Endogenous	FP-tagged	Protein function	References
PCNA	P12004	+	+	DNA replication/repair	Moldovan et al. 2007; Stucki et al. 2001
Mcm3	P25205	+	n.a.	DNA replication	Maiorano et al. 2006
Mcm7	P33993	+	n.a.	DNA replication	
Ku70	P12956	+	n.a.	DNA repair	Mahaney et al. 2009; Weterings and Chen 2007
DNA-PKcs	P78527	+	n.a.	DNA repair	
Cdc5L	Q99459	+	+	Pre-mRNA splicing, cell cycle control	Ajuh et al. 2000, 2001; Boudrez et al. 2000
PLRG1	O43660	+	n.a.	Pre-mRNA splicing	Ajuh et al. 2000, 2001; Rappsilber et al. 2002
Prp19	Q9UMS4	+	n.a.	DNA repair, pre-mRNA splicing, E3 ligase activity, interactor with 20S proteasome	Grillari et al. 2005; Loscher et al. 2005; Mahajan and Mitchell 2003; Zhang et al. 2005
SF2/ASF	Q07955	+	n.a.	Pre-mRNA splicing	Zuo and Manley 1993
U2AF65	P26368	+	n.a.	Pre-mRNA splicing	Rappsilber et al. 2002
U1/U2 snRNP	–		n.a.	Pre-mRNA splicing	Lyon et al. 1997
Sm proteins (Y12 antibody)	–	+	+ (SmB)	Pre-mRNA splicing	Sleeman and Lamond 1999
PPM1G/PP2Cγ	Q6IAU5	+	+	Ser/Thr phosphatase, histone exchange factor, pre-mRNA splicing	Kimura et al. 2006; Murray et al. 1999; Petri et al. 2007; Travis and Welsh 1997
PNUTS/p99	Q96QC0	+	+	Inhibitor of protein phosphatase 1, DNA damage response	Kreivi et al. 1997; Landsverk et al. 2010
CRM1	O14980	+	+	Protein transport, intranuclear transport of snRNPs	Hutten and Kehlenbach 2007; Sleeman 2007
PA28γ/PSME3	P61289	+	+	Proteasome activator, UV-stress response of CBs, controls PML body number, chromosomal stability	Chen et al. 2007; Cioce et al. 2006; Zannini et al. 2008, 2009
20S proteasome	–	+	n.a.	Protein turnover	Gallastegui and Groll 2010
Coilin	P38432	+	+	Component of Cajal bodies	Gall 2000; Ogg and Lamond 2002
SUMO1	P63165	+	+	PTM	Geiss-Friedlander and Melchior 2007; Meulmeester and Melchior 2008; Ulrich 2009
SUMO2/3	P61956/ P55854	+	+	PTM	
TRIM28/KAP-1	Q13263	+	n.a.	Transcriptional co-repressor	Urrutia 2003
Trimethylguanosine cap (TMG)	–	+	n.a.		Andersen and Zieve 1991

"+" identified, *n.a.* not analysed

found within the INB (data not shown). No intranucleolar SUMO2 was found in differentiated fibre cells (data not shown), indicating that this reflects a cell feature characteristic of the epithelial layer. Additionally, we could detect an INB for SUMO1 in skin epithelial cells (Supplementary Figure S1).We conclude that the presence of the INB in tissue suggests it may have a physiological role in primary cells. Therefore, we pursued further analysis using the cell culture system.

Highly purified preparations of nucleoli can be isolated from cultured cells. By using the YFP-SUMO1 stable cell line, we monitored each fractionation step for the presence of the SUMO1-INB by fluorescence microscopy (data not shown). When these purified nucleoli were analysed as 200 nm cryo-sections by SEM, we observed cavities of varying size (Fig. 2a). The same nucleoli were subjected to immunogold staining for SUMO1 and TEM as 70 nm cryo-sections. Gold particles were found enriched around the edges as well as within of nucleolar cavities (Fig. 2b, c, arrowheads). This suggests that the cavities may correspond to the INB observed by fluorescence microscopy in intact cells.

The intranucleolar body is a dynamic compartment

The nucleolus is a dynamic organelle with many proteins either shuttling between the nucleolus and nucleoplasm (Tsai and McKay 2005) or else trafficking through it as part

Table 2 Frequency of the intranucleolar body (INB) for PA28γ in different cell lines

Cell line	Tissue of origin (species)	Number of experiments	Cells with INB [%]	STD [%]
293	Kidney (human)	3	6.3	±1.7
C33A	Cervix (human)	3	16.0	±5.8
CHO	Ovary (hamster)	3	16.9	±4.0
HaCaT	Skin (human)	3	14.0	±2.8
HCT116	Colon (human)	3	10.9	±4.6
HepG2	Liver (human)	3	20.1	±3.9
HT1080	Connective tissue (human)	3	10.4	±1.9
MCF7	Breast (human)	4	32.4	±10.0
Tera-1	Testes (human)	3	8.3	±4.7
U138	Brain (human)	2	9.1	±5.2
U2OS	Bone (human)	3	10.2	±2.8

A minimum of 100 cells per experiment was evaluated for the presence of the INB by double labelling for PA28γ and nucleolin

STD standard deviation

of their maturation pathway (reviewed in Gerbi et al. (2003)) or altering their association in response to metabolic conditions (Andersen et al. 2005). To analyse whether INB components exchanged with surrounding nucleoplasmic protein populations, we analysed different GFP-fusion proteins by FRAP following transient transfection. Different INB components displayed different dynamic behaviour (Fig. 3a, b). For example, when either GFP-PA28γ or GFP-PPM1G was photobleached, the intranucleolar pool recovered within ~1 min. The turnover of these proteins was so high that the recovery already started during the bleaching event. In contrast, intranucleolar GFP-SUMO1 or GFP-SUMO2/3 could be efficiently bleached and did not recover within the same time frame, indicating that compared with either PA28γ or PPM1G, a large portion of SUMO within the nucleolus exchanges only slowly (Fig. 3a, b for SUMO1 and data not shown). In contrast to this nucleolar population, GFP-tagged SUMO1 and SUMO2/3 in the nucleoplasm recovered within seconds after the bleach (data not shown). This is in agreement with earlier data, showing different dynamics of the SUMO paralogues in different subnuclear compartments (Ayaydin and Dasso 2004). Similar results were obtained with HeLa cells stably expressing either YFP-SUMO1 or YFP-SUMO2/3 (data not shown). By time-lapse imaging, we observed intranucleolar SUMO1 recovered eventually within ~30–60 min after the initial bleach, demonstrating that SUMO1 within the nucleolus is turned over slowly.

Fusions with photoconvertable fluorescent proteins (e.g. Dendra2) allow observation of a locally defined subpopulation of the protein of interest and the analysis of its dynamic behaviour over time (Chudakov et al. 2007).

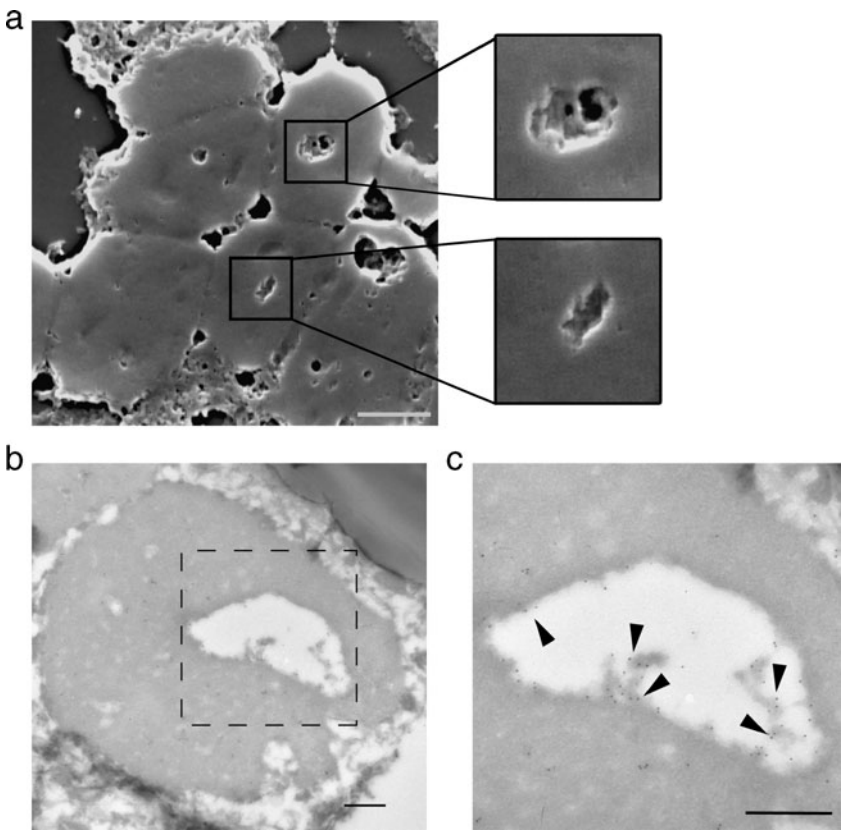

Fig. 2 The intranucleolar body by EM. Nucleoli purified from HeLa cells stably expressing EYFP-SUMO1 were analysed as 200-nm cryo-sections by scanning electron microscopy (**a**) and as 70-nm cryo-sections for immunoelectron microscopy in the transmission electron microscope using antibodies against SUMO1 and secondary antibodies conjugated to 10-nm immunogold (**b**, **c**). *Scale bars*, 1 μm in **a** and 100 nm in **b**, **c**. In **c**, a magnification of the intranucleolar immunogold labelling from the nucleolus in **b** is shown. Immunogold labelling for SUMO1 is indicated by *arrowheads*

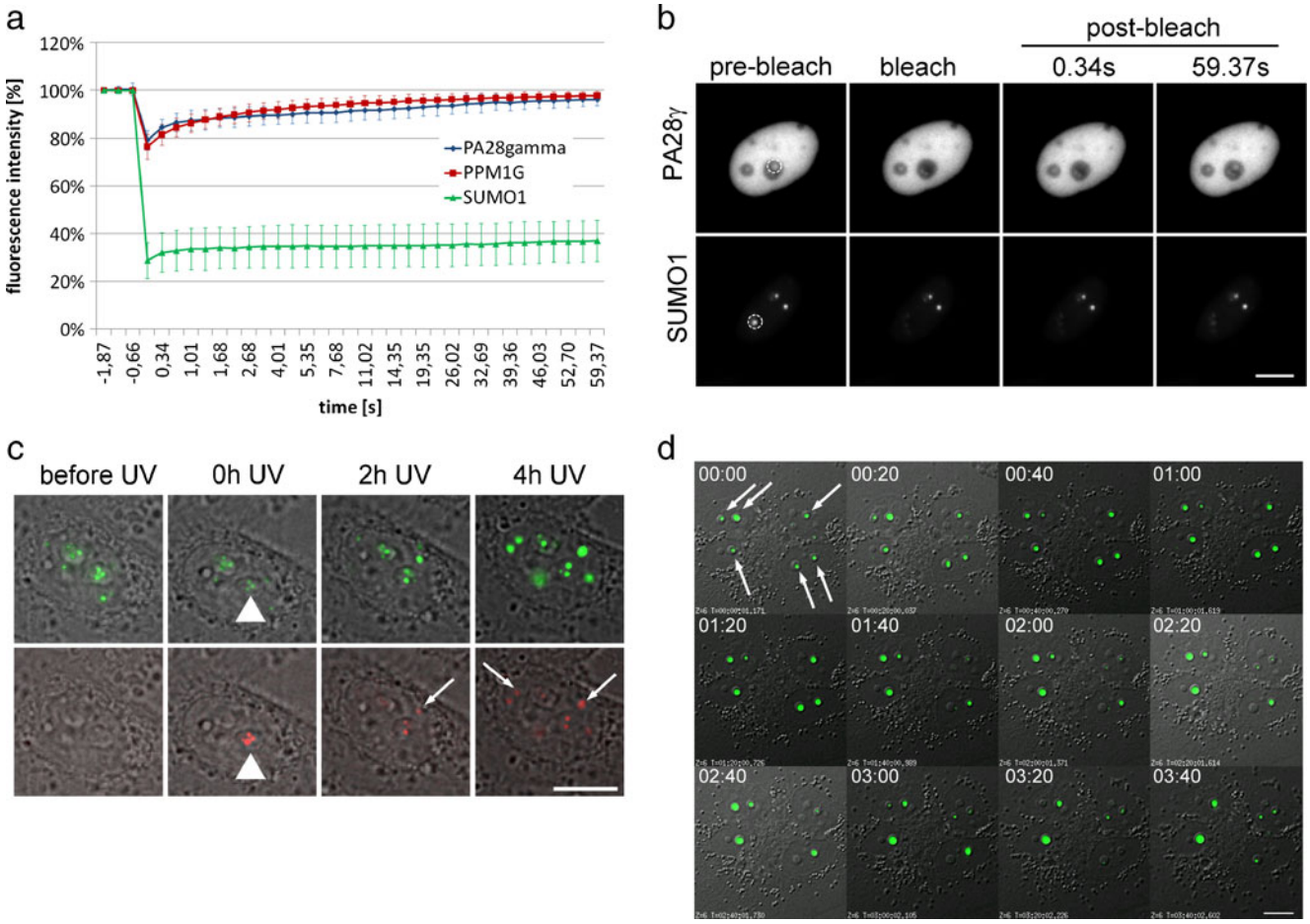

Fig. 3 Dynamics of the intranucleolar body. **a**, **b** FRAP analysis of HeLa cells transiently expressing either GFP-SUMO1, -PA28γ or PPM1G. The normalized, average recovery curves of the intranucleolar body with standard deviation of at least 20 individual cells are shown in **a**. A representative cell expressing either GFP-PA28γ (*top*) or GFPSUMO1 (*bottom*) is shown at the time directly before (pre-bleach), at the moment of bleach (bleach) and at two time points after the bleach (post-bleach; **b**). The bleached region is indicated (*circle*). *Bar*, 10 μm. **c** Time-lapse microscopy of the intranucleolar body for Dendra2-SUMO1 in HeLa cells before (before UV) and after photoconversion (0–4 h UV) with a 405-nm laser (UV). Non-photoconverted Dendra-Sumo2 (*green*, *top*) and photoconverted Dendra2-SUMO1 (*red*, *bottom*, indicated by *arrowhead*) are shown as merge with bright-field images acquired by Koehler illumination. Photoconverted Dendra-SUMO1 populations appearing in the nucleoplasm are indicated by *arrows*. *Bar*, 10 μm. **d** HeLa cells transiently expressing GFP-SUMO1 were analysed over time by time-lapse microscopy. A merge of the fluorescence image DIC is shown. Time in shown in hours:minutes. INBs are indicated (*arrows*). *Bar*, 10 μm

Dendra2-SUMO1 localises like GFP-SUMO1 to the INB as well as nucleoplasmic PML bodies (Fig. 3c). Dendra2-SUMO1 within the INB was photoconverted into its red isoform (arrowhead in Fig. 3c) using a 405-nm laser and subsequently analysed by time-lapse microscopy. Approximately 2 h after photoconversion of the nucleolar SUMO1, red foci appeared in the nucleoplasm (arrows in Fig. 3c). They increased in size as well as in intensity over time while the red foci in the nucleolus decreased. Neighbouring cells expressing Dendra2-SUMO1 that had not been photoconverted by the laser did not exhibit any red foci at the end of the experiment, confirming these nucleoplasmic foci derived from the converted nucleolar protein pool. These results show that the nucleolar SUMO1 constantly exchanges with other nuclear compartments, but with a low rate.

Due to the different optical density of the surrounding nucleolar material, the INB can also be visualized by differential interference contrast microscopy (DIC), appearing as a distinct, round structure within the nucleolus. Fluorescence imaging of HeLa cells transiently expressing GFP-SUMO1 confirms the presence of GFP-SUMO1 within this INB detected by DIC (Fig. 3d (arrows) and Supplementary Movies 1, 2, 3 and 4). Within the time frame of a few hours, the INB exhibited surprisingly dynamic macroscopic behaviour. It appeared to vary in size, either by fusion of several small structures into one larger INB or by shrinking. Occasionally, a short-term increase in the nucleoplasmic fluorescence for SUMO1 accompanied the disappearance of the INB, suggesting the release of its content into the nucleoplasm (see Movie 2 in

Supplementary Data). The INB did not appear to originate from nucleoplasmic invaginations, suggesting it forms within the nucleolus. These data indicate that the INB is not a rigid part of the nucleolar architecture, but rather appears and disappears periodically. We therefore sought to find conditions that either favour or inhibit its formation.

Induction of the intranucleolar body by specific DNA damaging agents

We next analysed the response of the INB to different stress treatments. IR is known to induce DNA DSBs, leading to the formation of phosphorylated H2AX-foci (γH2AX) at the site of DSBs (Fig. 4c, left panel). HeLa cells were exposed to an IR-dose of 10 Gy, left to recover for 3 h and subsequently analysed by indirect immunofluorescence for the presence of the INB. As exemplified for PA28γ (Fig. 4a, b) and His-SUMO1 (Supplementary Figure S2a, b), the percentage of cells showing an INB was increased after IR treatment. Whereas ~40% (PA28γ) and ~30% (His-SUMO1) of cells displayed an INB under non-stressed conditions, this frequency increased to ~75% upon IR for PA28γ and ~60% for His-SUMO1. We also noticed an increase in the average size of the INB (data not shown). The maximum percentage of cells displaying an INB was reached at ~3 h after irradiation and maintained up to ~10 h until cells started to recover at 12–24 h (data not shown).

To test whether the formation of an INB is promoted by a specific response to DSBs or by DNA damage in general, we tested whether other DNA-damaging agents had the same effect. Short-term treatment with the topoisomerase II inhibitor etoposide as well as prolonged incubation with either the topoisomerase I inhibitor camptothecin (CPT) or the replication fork stalling agent hydroxyurea (HU) have been described to result in DSBs upon DNA replication (Lundin et al. 2002; Ryan et al. 1991; Long et al. 1985). These treatments also induce the phosphorylation of H2AX (Fig. 4c, left panel; Supplementary Figure S2d). HeLa cells were incubated either for 3 h in the presence of 50 μM etoposide (eto) or for 24 h in the presence of either 25 nM CPT or 2 mM HU, and analysed by indirect immunofluorescence. All reagents caused a significant increase in the number of cells displaying an INB for either PA28γ or His-SUMO1 (Fig. 4b and Supplementary Figure S2b). Similar results were obtained for other INB components, including CDC5L and PPM1G, suggesting this stress-induced increase reflects a common cellular response shared by other components of the INB (data not shown). In contrast to IR, CPT or HU treatment, UV-C treatment did not result in an increase, but rather in a reduction, of the number of cells exhibiting an INB (Fig. 4b and Supplementary Figure S2b). UV-C irradiation does not result in DSB but in covalent adducts between adjacent pyrimidines on the DNA strands (cyclobutane pyrimidine dimers (CPDs); Tornaletti and Pfeifer 1996; Fig. 4c, right panel). Similar results were obtained using the UV-mimetic 4-nitroquinoline 1-oxide (NQO; Fig. 4b and Supplementary Figure S2b; Al-Baker et al. 2005; Tanooka and Tada 1975). This might indicate that the formation of the INB is triggered only by distinct types of DNA damage, such as DSBs and/or stalled replication forks, and therefore reflects a specific stress response by the cell.

Alternatively, the formation of the INB might be a consequence of a cell cycle arrest caused by the different DNA-damaging agents. Therefore, we analysed the cell cycle distribution of HeLa cells treated with either IR, eto, CPT or HU. The different stress treatments resulted in different cell cycle distributions (Supplementary Figure S3a–d). Whereas IR and etoposide treatment seemed to arrest cells in S and G2 phase, CPT and HU treatment arrested cells in G2 or late G1/early S phase, respectively. As about a third of unstressed HeLa cells display an INB, we set out to analyse the frequency of the INB during an unperturbed cell cycle. To avoid involvement of any drugs that might influence the abundance of the INB, we used CCE to collect HeLa cells in G1 phase. G1 cells were allowed to re-settle and were analysed at different time points after CCE for abundance of the INB in different cell cycle stages. Interestingly, 12 h after CCE with most cells being in S phase (see Supplementary Figure S3e), ~71% of cells (±10.5%) displayed an INB for PA28γ. When cells progressed into G2 phase (18 h after CCE), this number decreased to ~55% (±8.8%). In contrast, only ~19% (±3.6%) of cells in G1 phase (2 h after CCE) contained an INB for PA28γ. The low abundance of the INB during G1 was confirmed by analysis of cells after nocodazole release (data not shown) and is therefore unlikely to be an artefact of the CCE. These data indicate that the INB is prevalent in cells in S and G2 phase of an unperturbed cell cycle. The induced formation of the INB by specific DNA-damaging agents therefore could reflect either cells arrested in S phase and/or cells that have retained the INB after exit from S phase into G2 due to DNA damage.

Recently, an accumulation of p21 in the nucleolus has been reported at sites distinct from the localisation of nucleolar markers seen upon DNA damage by UV or adriamycin (Abella et al. 2010). This was accompanied by a segregation of the fibrillar and granular components and by formation of nucleolar caps as a result of transcriptional inhibition. To analyse whether the INB might be induced by similar mechanisms, we examined the effect of IR irradiation on nucleolar architecture and function. No change was observed in the localisation of UBF and Nop58, as marker for the FC and DFC, respectively, after 3 h of recovery from IR (Fig. 5a). This was also true either at shorter (5 min to 1 h) and longer recovery periods (up to

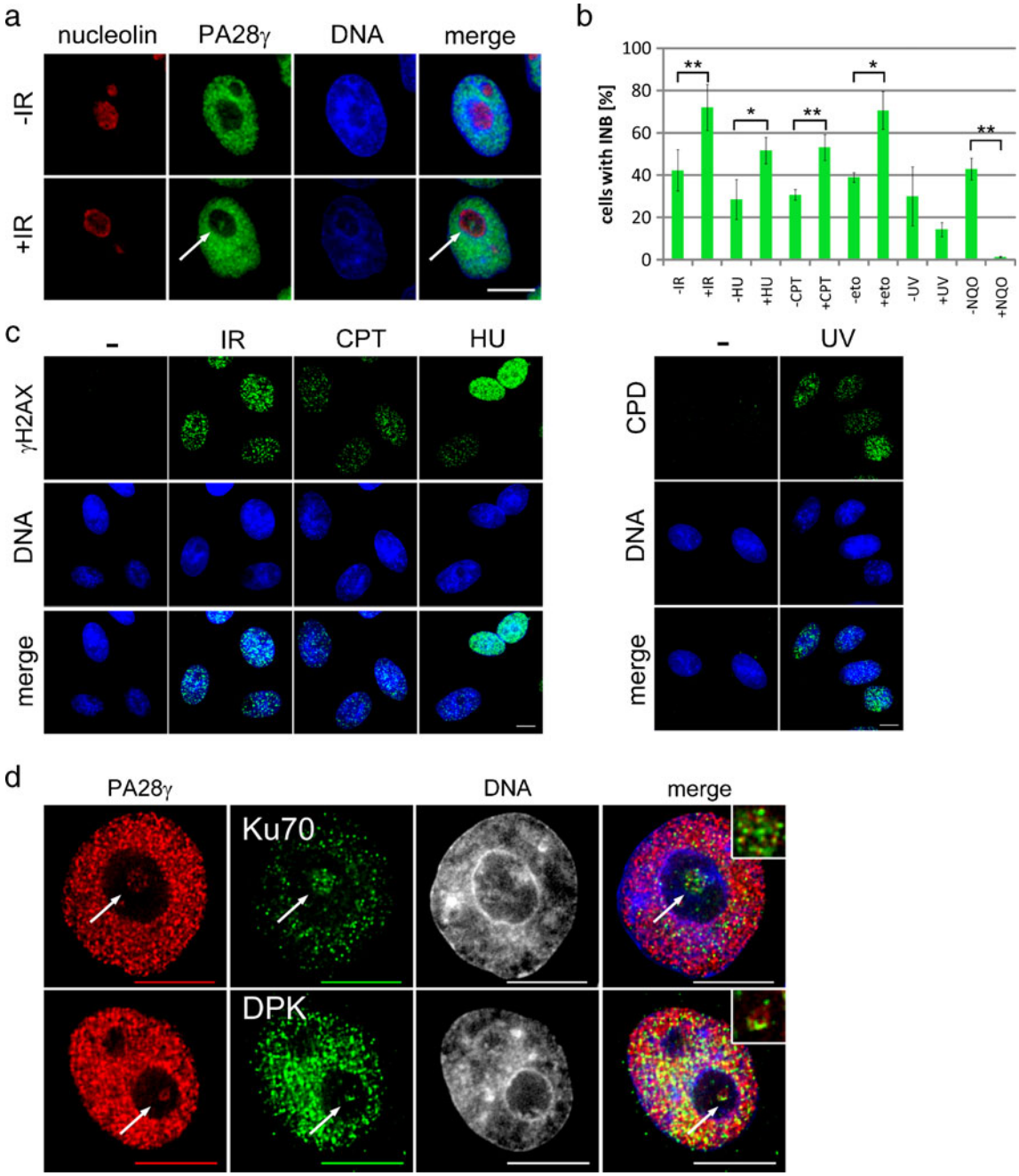

Fig. 4 The intranucleolar body is induced by specific types of DNA-damage. **a** Untreated HeLa cells (−IR) or cells 3 h after exposure to 10 Gy (+IR) were analysed by co-immunofluorescence for PA28γ and nucleolin. The INB is indicated by an *arrow*. *Bar*, 10 μm. **b** Quantification of HeLa cells displaying an intranucleolar body for endogenous PA28γ after various stress treatments. *Error bars* represent the standard deviation of $n=5$ (IR, 3 h recovery), $n=3$ (HU, eto, UV, NQO) and $n=4$ (CPT) independent experiments with >100 cells evaluated each. *p* values were determined using a heteroscedastic, two-tailed *t* test and are indicated as *single asterisk* for $p \leq 0.05$ (significant) and *double asterisk* for $p \leq 0.01$ (highly significant). **c** Immunofluorescence for γH2AX (*left panel*) of untreated (−), γ-irradiated (IR), camptothecin (CPT) or hydroxyurea (HU)-treated HeLa cells. The *right panel* shows an immunofluorescence for cyclobutane pyrimidine dimers (CPD) in either untreated HeLa cells (−) or cells exposed to UV-C (UV). **d** HeLa cells were treated with 25 nM CPT for 24 h and double labelled with antibodies for endogenous PA28γ and either Ku70 (*upper panel*) or DPK (*lower panel*). *Arrows* point to the localisation of the INB. *Bar*, 10 μm

12 h) after IR, or in cells that were incubated for 24 h in the presence of either HU or CPT (data not shown). Treatment of cells with low doses of actinomycin D (actD, 5 nM for 3 h), to specifically inhibit RNA pol I activity, however, resulted in formation of nucleolar caps for both UBF and fibrillarin (Fig. 5a, lower panel).

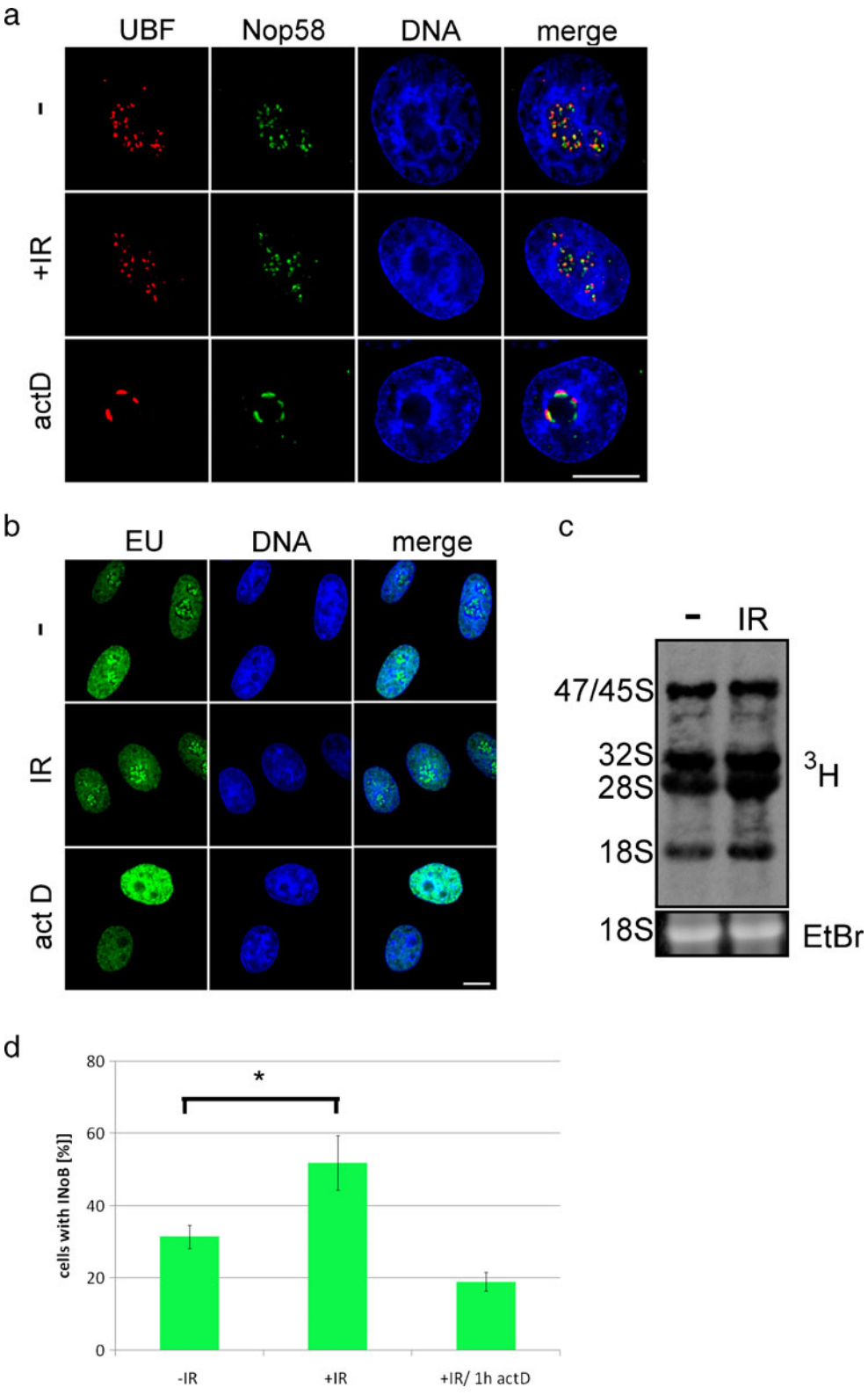

Fig. 5 Stress stimuli triggering the intranucleolar body do not interfere with nucleolar function. **a** HeLa cells were either left untreated, exposed to 10 Gy (3 h recovery) or treated for 3 h with 5 nM actinomycin D (actD) and subsequently analysed by immunofluorescence using antibodies against UBF and Nop58. *Bar*, 10 μm. **b** Untreated HeLa cells (−), cells exposed to 10 Gy (IR; 3 h recovery) or after 3 h of treatment with 5 nM actinomycin D (act D) were pulse-labelled with EU for 10 min and subsequently analysed by fluorescence microscopy. *Bar*, 10 μm. **c** Untreated HeLa cells (−) or cells 1 h after exposure to 10 Gy (IR) were pulse-labelled with [5,6-3H]uridine (3H) for 2 h, total RNA isolated and analysed by northern blot and subsequent autoradiography. The ethidium bromide stain (EtBr) of the total 18S rRNA is shown as a loading control. **d** Quantification of cells displaying an intranucleolar body for endogenous PA28γ in cells left untreated (−IR), 3 h after exposure to 10 Gy in the absence (+IR) or presence (IR/1 h act D) of 5 nM actinomycin D for 1 h. *Error bars* represent the standard deviation of three (−IR, +IR) or two (IR/actD) independent experiments with >100 cells each. The *p* value was determined using a heteroscedastic, two-tailed *t* test and is indicated as *single asterisk* for $p \leq 0.05$ (significant)

The preservation of nucleolar architecture upon IR treatment indicates ongoing transcriptional activity in the nucleolus. To address this directly, we labelled freshly synthesised RNA by pulse labelling with 5-ethynyl uridine (EU) and analysed the amount of EU incorporation by fluorescence microscopy. Due to the high transcription rate of rRNA, nucleoli appear strongly labelled compared with the nucleoplasm (Fig. 5b, control). We did not detect a

change in the level of transcription in IR-treated cells compared with control cells, confirming that irradiated cells were indeed transcriptionally active, as suggested by their normal nucleolar architecture. In contrast, treatment of cells with low doses of actD (5 nM) significantly reduced the level of EU incorporation specifically within the nucleoli without reduction in the rate of nucleoplasmic transcription (Fig. 5b).

In ribosomal biogenesis, the primary 47/45S rRNA transcript is processed into the final 28S, 18S and 5.8S rRNAs. So, even though cells are actively transcribing rRNA as determined by EU incorporation, the processing of the rRNA precursor might still be affected by IR. Therefore, we examined transcription and processing of rRNA in unstressed and irradiated cells by metabolic labelling with [5,6-^{3}H]-uridine and subsequent northern blot analysis. In agreement with the level of EU incorporation, no change in the amount of the primary 45/47S rRNA transcript could be observed upon IR (Fig. 5c). Furthermore, its processing into the 32S rRNA intermediate and final 28S and 18S rRNA products was not prevented by IR.

In conclusion, IR promotes the formation of the INB without disrupting nucleolar structure or function. This is in agreement with our observation that already a fraction of unstressed cells with normal nucleolar morphology appears to have an INB (Fig. 1a).

To analyse whether the presence of the INB in turn depends on nucleolar transcription activity, we compared untreated cells with irradiated cells that were additionally incubated for 1 h in the absence or presence of low doses of actinomycin D to specifically inhibit RNA pol I. The IR-induced formation of the INB was abolished by the short inhibition of RNA pol I transcription (Fig. 5d). Longer incubation of either irradiated, or untreated, cells with actinomycin D (up to 3 h) led to loss of the INB (data not shown), suggesting that it is dependent on intact nucleolar structure and/or nucleolar transcription.

The intranucleolar body is in close proximity to ribosomal DNA

During our analysis, we noticed the presence of a DNA fibre, either in close proximity to, or, in some cases, wrapped around the INB. Nucleoli are known to form around rDNA repeats, but other chromatin regions are also known to associate with the nucleolus in mammalian cells, such as telomeres, centromeres and other recently identified ‘nucleolar-associated domains’ (NADs; Carvalho et al. 2001; Haaf and Schmid 1989; Manuelidis 1984; Manuelidis and Borden 1988; Nemeth et al. 2010; Ochs and Press 1992; van Koningsbruggen et al. 2010). To determine whether these intranucleolar DNA fibres associated with the INB correspond to rDNA, we combined DNA-FISH for rDNA with immunostaining for SUMO1 to detect the INB and immunolabelling for the known rDNA binding protein UBF in HeLa cells stably expressing His-SUMO1. The rDNA probe labelled nucleoli, demonstrating the specificity of the hybridization. When individual *z*-stacks of cells displaying the intranucleolar SUMO1-body were analysed, the rDNA-probe labelled the DNA fibre directly beside the INB (arrows in Fig. 6a, top panel). The same result was obtained using antibodies specific for either endogenous PA28γ (Supplementary Figure S4a), or an rDNA probe specific for a different rDNA region (data not shown). Other nucleolar-associated DNA domains (NAD), such as the telomeres on the short arm of chromosome 4 (van Koningsbruggen et al. 2010), did not exhibit close proximity to the INB, demonstrating that we were able to distinguish individual NADs spatially even in a confined space such as the nucleolus (Supplementary Figure S4a). This association was also preserved under conditions that promote formation of the INB, such as IR or CPT treatment (Fig. 6a, lower panel and data not shown). Transcription of rDNA accounts for the majority of cellular transcription. Having identified a number of factors involved in RNA splicing within the nucleolar body (see Table 1), we wondered whether they were involved in rRNA transcription and/or processing. However, when we labelled nascent RNA by EU incorporation, we could not detect any co-localisation with the INB (as shown for PA28γ in Fig. 6b), suggesting that the INB may not be a site of either rRNA transcription or processing.

UBF is an rDNA transcription factor that is involved in establishing a euchromatic state of rDNA (reviewed in McStay and Grummt (2008) and Sanij and Hannan (2009)). No co-localisation of the INB with either UBF or RNA pol I (RPA194), both markers for the FC, could be observed (see Figs. 1a and 6a). In fact, the SUMO1-nucleolar body and UBF mostly appeared mutually excluded on rDNA (Fig. 6a).

Next, we tested whether the INB might be associated with transcriptionally silent, heterochromatic DNA. Eu- and heterochromatic DNA can be distinguished by specific histone modifications, such as lysine 9 trimethylated histone H3 (H3K9me3) or lysine 20 trimethylated histone H4 (H4K20me3) for heterochromatin and lysine 16 acetylated histone H4 (H4K16ac) or lysine 36 trimethylated histone H3 (H3K36me3) for euchromatin (Bannister et al. 2001, 2005; Shogren-Knaak and Peterson 2006; Vakoc et al. 2006; Schmitz et al. 2010; Schotta et al. 2004). By immunofluorescence, we found the heterochromatin markers H3K9me3 and H4K20me3 directly adjacent to the INB stained for PA28γ (Fig. 6c and Supplementary Figure S4b, top panel, indicated by arrows). The euchro-

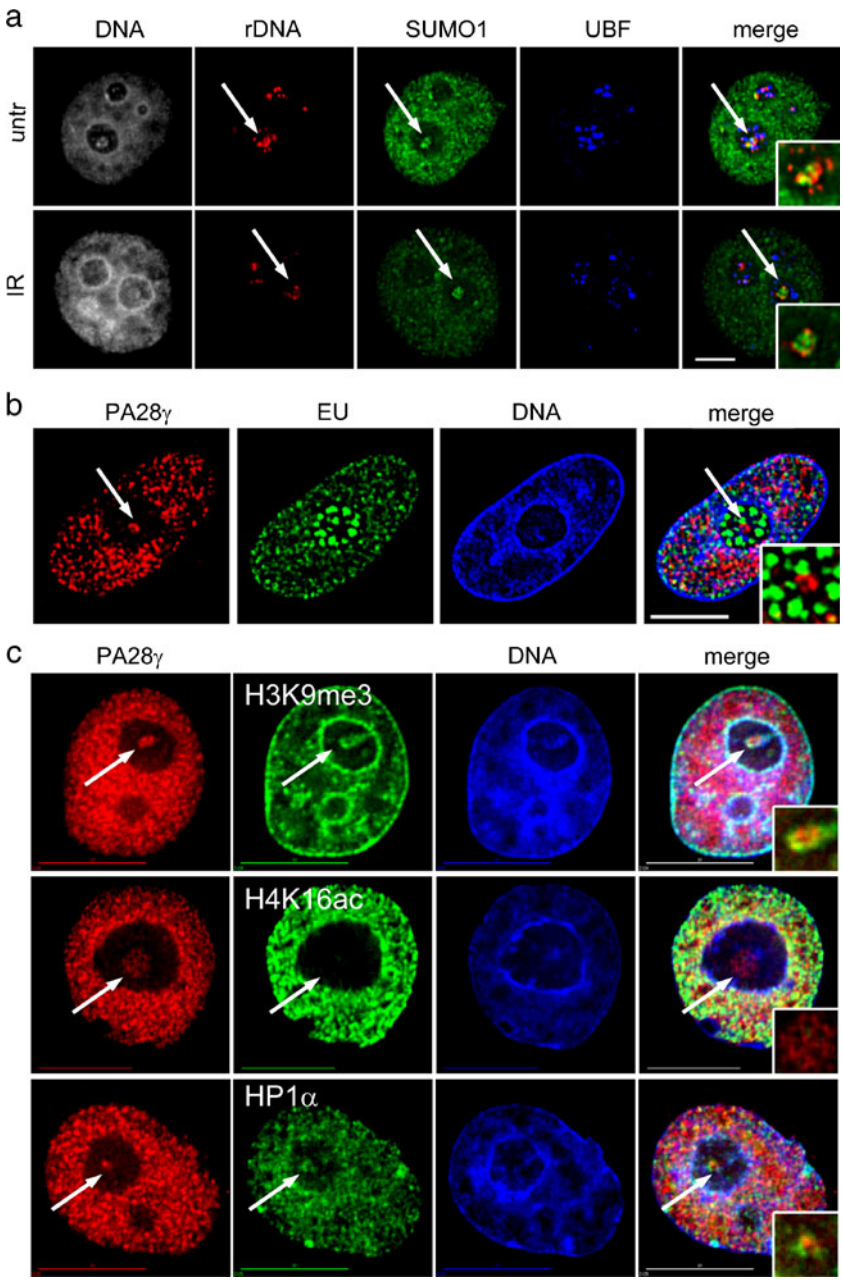

Fig. 6 The intranucleolar body is associated with transcriptionally silent ribosomal rDNA (rDNA). **a** Untreated HeLa His-SUMO1 cells (*untr*) or cells 6 h after exposure to 10 Gy (IR) were analysed by combined FISH for rDNA and immunofluorescence for SUMO1 and UBF. The DNA and UBF stain were omitted in the *insets*. An *arrow* points towards the INB with associated rDNA. **b** HeLa cells were subjected to 10 min pulse-labelling with EU, and subsequently analysed by indirect immunofluorescence using antibodies for PA28γ. The INB for PA28γ is indicated (*arrow*). **c** HeLa cells were subjected to double immunofluorescence for PA28γ and trimethylated lysine 9 histone H3 (H3K9me3) (top), lysin16 acetylated histone H4 (H4K16ac; *middle panel*) or HP1α (*bottom*), respectively. The DNA stain was omitted in the *insets*. *Arrows* point towards the localisation of the INB. *Bar*, 10 μm

matic marker H4K16ac, however, was excluded from this intranucleolar DNA fibre and not found near the INB (Fig. 6c, middle panel). Proteins involved in gene repression, such as the heterochromatin protein 1 (HP1), are known to be recruited by histone modifications such as H3K9me3 (Bannister et al. 2001; Lachner et al. 2001; Nakayama et al. 2001). As shown in Fig. 6c (arrows in lower panel), HP1α localises adjacent to the INB. Also, the transcriptional co-repressor TRIM28 can be found together with PA28γ in the INB (Supplementary Figure S4b, lower panel), further supporting the hypothesis that the INB might be associated with transcriptionally silent rDNA.

Discussion

In this study, we identify 22 factors, encompassing 21 proteins and one RNA component (TMG), in a subnucleolar region that is not directly associated with sites of rRNA synthesis. For a few proteins, this intranucleolar localisation has been observed before, e.g. for SUMO1, CRM1, CDC5L, coilin and splicing snRNPs (Ajuh et al. 2001; Desterro et al. 2005; Ernoult-Lange et al. 2009; Lyon et al. 1997; Sleeman et al. 1998; Sleeman and Lamond 1999); however, the conditions of their intranucleolar localisation and dynamics have not been characterized in detail. Importantly, despite the presence of the Cajal body marker coilin in the INB, the level of coilin

within the INB does not correspond to the locally high concentration of coilin seen accumulated in Cajal bodies. Rather, the level of coilin in the INB is similar to the nucleoplasm. Furthermore, many of the factors detected in the INB are not present in Cajal bodies. Therefore, we exclude that the INB corresponds to Cajal bodies within the nucleolus.

Some of the factors localized to the INB are known to either interact directly, or else to be part of the same protein or RNP complex, for example, PA28γ with the 20S proteasome, CDC5L, PLRG1 and Prp19 within the CDC5L complex and TMG-capped snRNAs with snRNPs (Ajuh et al. 2000; Andersen and Zieve 1991; Mao et al. 2008). These constituents of the INB are involved in diverse functions including the cellular stress response to DNA damage, DNA replication, pre-mRNA splicing, protein turnover and chromatin organization. Several of these proteins are implicated in multiple cellular processes. For example, the Ser/Thr phosphatase PPM1G has been shown to influence the subcellular localisation of SMN, to act in pre-mRNA splicing, in dephosphorylation of coilin, histone H2B and γH2AX as well as in histone H2A/H2B exchange (Allemand et al. 2007; Hearst et al. 2009; Kimura et al. 2006; Murray et al. 1999; Petri et al. 2007). The CDC5L complex and its constituents CDC5L, PLRG1 and Prp19 have additionally been linked to the DNA damage response (Legerski 2009; Lu and Legerski 2007; Zhang et al. 2005, 2009).

Post-translational protein modifications with SUMO1 and SUMO2/3 are well known to have multiple roles, such as regulating protein activity, stability and/or subcellular localisation, and have also been linked to rDNA maintenance (reviewed in Eckert-Boulet and Lisby (2009) and Geiss-Friedlander and Melchior (2007)). We recently reported a proteomic screen for SUMOylated proteins within the nucleolus, demonstrating a role for SUMOylation of Nop5/Nop58 in the regulation for snoRNP biogenesis (Westman et al. 2010). However, if snoRNP proteins are the major targets for SUMOylation in the nucleolus, they mainly localise in the DFC and do not co-localise with the INB (data not shown). In the future, it will be interesting to identify the SUMOylated proteins within the INB and to determine their function within the nucleolus.

We were also able to detect SUMO1 by immuno-EM in the INB within purified nucleoli. Here, they associated with nucleolar cavities. As we were not able to observe these cavities by EM of nucleoli in unfractionated intact cells, the INB might either represent an area of reduced structural stability compared to other nucleolar compartments or, alternatively, may be obscured by components that were lost during nucleoli purification.

Recently, an intranucleolar localisation different to FC, DFC or GC was described upon MG132 or adriamycin treatment for p53 and p21, respectively (Abella et al. 2010; Kruger and Scheer 2010; Latonen et al. 2010). However, both these treatments interfere with the integrity and/or function of the nucleolus. MG132 has been described to cause either nucleolar aggregates and/or nucleoplasmic invaginations into the nucleolus (Kruger and Scheer 2010; Latonen et al. 2010), whereas adriamycin treatment, like UV-irradiation, results in inhibition of rRNA synthesis and nucleolar cap formation (Abella et al. 2010). Importantly, the INB we observe is a feature of intact and functional nucleoli. In contrast to p21 or p53, the components of the INB detected in this study are continuously expressed and are located within the INB of unstressed cells, albeit with a lower frequency. Also, neither nucleolar structure nor ribosome subunit biogenesis are prevented by stress treatments that promote formation of the INB. Of course, we cannot exclude an influence of the DNA-damaging agents on the nucleolus, which cause little change to its architecture and functionality but that might indirectly trigger the formation of the INB.

We were able to show that formation of the INB is dependent on a functional nucleolus because inhibition of RNA pol I transcription by short-term treatment with low doses of actinomycin D abolished INB formation upon DNA damage. A basal transcriptional activity has been suggested to occur in nucleoli of hibernating dormice, which have been shown to contain coilin located in an INB (Malatesta et al. 2000). These results are consistent with the data obtained in lens tissue, as the epithelial cell layer that contains an INB has been shown to be transcriptionally active at a low level, whereas differentiated fibre cells, which do not exhibit an INB, are either transcriptionally highly active (early differentiated fibre cells) or transcriptionally silent (late fibre cells). Therefore, the INB we describe here may be different to the intranucleolar localisation described for p53 and p21. Our data however agree with the recent report of the presence of subnucleolar bodies containing CRM1, whose presence is dependent on ongoing RNA pol I activity (Ernoult-Lange et al. 2009). However, in contrast to CRM1, localisation of other components to the INB could not be inhibited by the drug leptomycin B (LMB), suggesting their recruitment occurs independently of CRM1 (Ernoult-Lange et al. 2009; own observation).

Interestingly, different components within the INB appeared to have distinct turnover rates when analysed by FRAP. In contrast to the highly mobile INB components PA28γ and PPM1G (recovery within ~1 min), SUMO-conjugated proteins exhibited a very low (though measurable) mobility. This result indicates that the INB likely does not represent protein aggregates, such as those described for nuclear proteins within the nucleolus upon proteasome inhibition (Latonen et al. 2010).

The observation that the INB is mostly abundant in cells during S phase, localises in close proximity to rDNA and is promoted by specific DNA damaging agents might indicate that, at least in part, its components are linked to the maintenance of rDNA repeats. As shown in Table 1, we identified several proteins within the INB that are implicated in DNA repair, such as DNA-PK, Ku70, PCNA and components of the CDC5L complex. Interestingly, replication of rDNA repeats in *Saccharomyces cerevisiae* has been shown to involve stalled replication forks as part of the regular replication mechanism, and this has been suggested to lead to increased recombinational activity within the rDNA locus (Brewer and Fangman 1988; Kobayashi et al. 1998; Linskens and Huberman 1988). Also, it has been recently reported that maintaining integrity of rDNA is very important because deletion of rDNA repeats affects nucleolar structure, alters the balance between genomic eu- and heterochromatin in *Drosophila*, and changes lifespan in yeast by mechanisms involving DNA recombination and repair (Paredes and Maggert 2009; Prokopowich et al. 2003). Therefore, the periodic appearance and disappearance of the INB (Fig. 3d) might indicate a basal level of DNA repair for rDNA gene arrays in unstressed cells during the cell cycle. The presence of several markers for heterochromatic and transcriptionally silent DNA, such as H3K9me3, H4K20me3 and HP1α on the rDNA associated with the INB and the transcriptional co-repressor TRIM28 within the INB, could potentially indicate the rDNA repeats are transcriptionally repressed. However, histone modifications such as H3K9me3 have also been described to occur in active genes, preventing a precise conclusion about the transcriptional activity of these rDNA repeats. Moreover, it is well possible that the INB might serve more than one function. Many proteins found within the INB are not known to be involved in the DNA damage response or chromatin organisation, such as SF2 or CRM1. We also observed a drastic reduction of the INB by staining for PA28γ upon reduced snRNP assembly, caused by RNAi-mediated depletion of SMN (data not shown). These issues therefore require further investigation.

Additionally to its association with rDNA, the presence of the INB can be abolished by treatment of cells with actD. It is therefore possible that DNA damage is dependent upon active transcription of rDNA genes. As inhibition of RNA pol I activity also interferes with nucleolar structure; we are not able to distinguish whether the INB is primarily dependent on ongoing transcription and/or nucleolar integrity. It would also be interesting to test whether the formation of the INB is dependent on existing heterochromatin, or even is involved in its formation.

Acknowledgements From the University of Dundee, we thank Sam Swift, Calum Thomson and the microscopy facility for technical support and assistance; Rosemary Clark (flow cytometry), Fabio Avolio for the GFP-PPM1G construct, Jonathon Chubb for the pHRS-7.1EcoRI rDNA probe, John Rouse and Ivan Munoz for reagents and advice regarding DNA damage; Manjula Nagala for help with rRNA analysis and Nicola Cook for technical assistance with the tissue staining. We are grateful to Ron Hay for his generous support with sheep anti-SUMO1 and anti-SUMO2/3 antibodies, the GFP-SUMO1 and -SUMO2/3 constructs as well as the HeLa His-SUMO1 cells. We additionally thank Brian McStay (University of Galway, Galway, Ireland) for the 11.9 rDNA probe, Archa Fox (Western Australia Institute for Medical Research, Perth, Australia) for pcDNA-mCherry and Julie Woods (Ninewells Hospital, Dundee, UK) for the anti-CPD antibody. We thank all members of the Lamond laboratory for their advice and suggestions. A.I.L. is a Wellcome Trust Principal Research Fellow. S.H. is supported by a postdoctoral Leopoldina Research Fellowship (BMBF-LPD 9901/8-177).

References

Abella N, Brun S, Calvo M, Tapia O, Weber JD, Berciano MT, Lafarga M, Bachs O, Agell N (2010) Nucleolar disruption ensures nuclear accumulation of p21 upon DNA damage. Traffic 11 (6):743–755. doi:10.1111/j.1600-0854.2010.01063.x

Ajuh P, Kuster B, Panov K, Zomerdijk JC, Mann M, Lamond AI (2000) Functional analysis of the human CDC5L complex and identification of its components by mass spectrometry. EMBO J 19(23):6569–6581. doi:10.1093/emboj/19.23.6569

Ajuh P, Sleeman J, Chusainow J, Lamond AI (2001) A direct interaction between the carboxyl-terminal region of CDC5L and the WD40 domain of PLRG1 is essential for pre-mRNA splicing. J Biol Chem 276(45):42370–42381. doi:10.1074/jbc.M105453200

Al-Baker EA, Oshin M, Hutchison CJ, Kill IR (2005) Analysis of UV-induced damage and repair in young and senescent human dermal fibroblasts using the comet assay. Mech Ageing Dev 126(6–7):664–672. doi:10.1016/j.mad.2004.12.002

Allemand E, Hastings ML, Murray MV, Myers MP, Krainer AR (2007) Alternative splicing regulation by interaction of phosphatase PP2Cgamma with nucleic acid-binding protein YB-1. Nat Struct Mol Biol 14(7):630–638. doi:10.1038/nsmb1257

Andersen J, Zieve GW (1991) Assembly and intracellular transport of snRNP particles. Bioessays 13(2):57–64. doi:10.1002/bies.950130203

Andersen JS, Lam YW, Leung AK, Ong SE, Lyon CE, Lamond AI, Mann M (2005) Nucleolar proteome dynamics. Nature 433 (7021):77–83. doi:10.1038/nature03207

Austin CM, Bellini M (2010) The dynamic landscape of the cell nucleus. Mol Reprod Dev 77(1):19–28. doi:10.1002/mrd.21088

Ayaydin F, Dasso M (2004) Distinct in vivo dynamics of vertebrate SUMO paralogues. Mol Biol Cell 15(12):5208–5218. doi:10.1091/mbc.E04-07-0589

Bannister AJ, Zegerman P, Partridge JF, Miska EA, Thomas JO, Allshire RC, Kouzarides T (2001) Selective recognition of methylated lysine 9 on histone H3 by the HP1 chromo domain. Nature 410(6824):120–124. doi:10.1038/3506513835065138

Bannister AJ, Schneider R, Myers FA, Thorne AW, Crane-Robinson C, Kouzarides T (2005) Spatial distribution of di- and tri-methyl lysine 36 of histone H3 at active genes. J Biol Chem 280 (18):17732–17736. doi:10.1074/jbc.M500796200

Boisvert FM, van Koningsbruggen S, Navascues J, Lamond AI (2007) The multifunctional nucleolus. Nat Rev 8(7):574–585. doi:10.1038/nrm2184

Boisvert FM, Lam YW, Lamont D, Lamond AI (2010) A quantitative proteomics analysis of subcellular proteome localization and changes induced by DNA damage. Mol Cell Proteomics 9 (3):457–470. doi:10.1074/mcp.M900429-MCP200

Boudrez A, Beullens M, Groenen P, Van Eynde A, Vulsteke V, Jagiello I, Murray M, Krainer AR, Stalmans W, Bollen M (2000) NIPP1-mediated interaction of protein phosphatase-1 with CDC5L, a regulator of pre-mRNA splicing and mitotic entry. J Biol Chem 275(33):25411–25417. doi:10.1074/jbc.M001676200

Boulon S, Westman BJ, Hutten S, Boisvert FM, Lamond AI (2010) The nucleolus under stress. Mol Cell 40(2):216–227. doi:10.1016/j.molcel.2010.09.024

Brewer BJ, Fangman WL (1988) A replication fork barrier at the 3' end of yeast ribosomal RNA genes. Cell 55(4):637–643

Carvalho C, Pereira HM, Ferreira J, Pina C, Mendonca D, Rosa AC, Carmo-Fonseca M (2001) Chromosomal G-dark bands determine the spatial organization of centromeric heterochromatin in the nucleus. Mol Biol Cell 12(11):3563–3572

Chen X, Barton LF, Chi Y, Clurman BE, Roberts JM (2007) Ubiquitin-independent degradation of cell-cycle inhibitors by the REGgamma proteasome. Mol Cell 26(6):843–852. doi:10.1016/j.molcel.2007.05.022

Chudakov DM, Lukyanov S, Lukyanov KA (2007) Using photo-activatable fluorescent protein Dendra2 to track protein movement. Biotechniques 42(5):553, 555, 557 passim

Cioce M, Boulon S, Matera AG, Lamond AI (2006) UV-induced fragmentation of Cajal bodies. J Cell Biol 175(3):401–413. doi:10.1083/jcb.200604099

Dahm R, Gribbon C, Quinlan RA, Prescott AR (1998) Changes in the nucleolar and coiled body compartments precede lamina and chromatin reorganization during fibre cell denucleation in the bovine lens. Eur J Cell Biol 75(3):237–246

Desterro JM, Keegan LP, Jaffray E, Hay RT, O'Connell MA, Carmo-Fonseca M (2005) SUMO-1 modification alters ADAR1 editing activity. Mol Biol Cell 16(11):5115–5126. doi:10.1091/mbc.E05-06-0536

Eckert-Boulet N, Lisby M (2009) Regulation of rDNA stability by sumoylation. DNA Repair 8(4):507–516. doi:10.1016/j.dnarep.2009.01.015

Ernoult-Lange M, Wilczynska A, Harper M, Aigueperse C, Dautry F, Kress M, Weil D (2009) Nucleocytoplasmic traffic of CPEB1 and accumulation in Crm1 nucleolar bodies. Mol Biol Cell 20 (1):176–187. doi:10.1091/mbc.E08-09-0904

Gall JG (2000) Cajal bodies: the first 100 years. Annu Rev Cell Dev Biol 16:273–300. doi:10.1146/annurev.cellbio.16.1.273

Gallastegui N, Groll M (2010) The 26S proteasome: assembly and function of a destructive machine. Trends Biochem Sci 35 (11):634–642. doi:10.1016/j.tibs.2010.05.005

Ganot P, Jady BE, Bortolin ML, Darzacq X, Kiss T (1999) Nucleolar factors direct the 2'-O-ribose methylation and pseudouridylation of U6 spliceosomal RNA. Mol Cell Biol 19(10):6906–6917

Geiss-Friedlander R, Melchior F (2007) Concepts in sumoylation: a decade on. Nat Rev 8(12):947–956. doi:10.1038/nrm2293

Gerbi SA, Lange TS (2002) All small nuclear RNAs (snRNAs) of the [U4/U6.U5] Tri-snRNP localize to nucleoli; identification of the nucleolar localization element of U6 snRNA. Mol Biol Cell 13 (9):3123–3137. doi:10.1091/mbc.01-12-0596

Gerbi SA, Borovjagin AV, Lange TS (2003) The nucleolus: a site of ribonucleoprotein maturation. Curr Opin Cell Biol 15(3):318–325

Gribbon C, Dahm R, Prescott AR, Quinlan RA (2002) Association of the nuclear matrix component NuMA with the Cajal body and nuclear speckle compartments during transitions in transcriptional activity in lens cell differentiation. Eur J Cell Biol 81(10):557–566

Grillari J, Ajuh P, Stadler G, Loscher M, Voglauer R, Ernst W, Chusainow J, Eisenhaber F, Pokar M, Fortschegger K, Grey M, Lamond AI, Katinger H (2005) SNEV is an evolutionarily conserved splicing factor whose oligomerization is necessary for spliceosome assembly. Nucleic Acids Res 33(21):6868–6883

Haaf T, Schmid M (1989) Centromeric association and non-random distribution of centromeres in human tumour cells. Hum Genet 81(2):137–143

Haaf T, Hayman DL, Schmid M (1991) Quantitative determination of rDNA transcription units in vertebrate cells. Exp Cell Res 193(1):78–86

Handwerger KE, Gall JG (2006) Subnuclear organelles: new insights into form and function. Trends Cell Biol 16(1):19–26. doi:10.1016/j.tcb.2005.11.005

Hearst SM, Gilder AS, Negi SS, Davis MD, George EM, Whittom AA, Toyota CG, Husedzinovic A, Gruss OJ, Hebert MD (2009) Cajal-body formation correlates with differential coilin phosphorylation in primary and transformed cell lines. J Cell Sci 122(Pt 11):1872–1881. doi:10.1242/jcs.044040

Huang S, Rothblum LI, Chen D (2006) Ribosomal chromatin organization. Biochem Cell Biol 84(4):444–449. doi:10.1139/o06-089

Hutten S, Kehlenbach RH (2007) CRM1-mediated nuclear export: to the pore and beyond. Trends Cell Biol 17(4):193–201

Kauffman MG, Noga SJ, Kelly TJ, Donnenberg AD (1990) Isolation of cell cycle fractions by counterflow centrifugal elutriation. Anal Biochem 191(1):41–46

Kimura H, Takizawa N, Allemand E, Hori T, Iborra FJ, Nozaki N, Muraki M, Hagiwara M, Krainer AR, Fukagawa T, Okawa K (2006) A novel histone exchange factor, protein phosphatase 2Cgamma, mediates the exchange and dephosphorylation of H2A-H2B. J Cell Biol 175(3):389–400. doi:10.1083/jcb.200608001

Kobayashi T, Heck DJ, Nomura M, Horiuchi T (1998) Expansion and contraction of ribosomal DNA repeats in *Saccharomyces cerevisiae*: requirement of replication fork blocking (Fob1) protein and the role of RNA polymerase I. Genes Dev 12 (24):3821–3830

Kreivi JP, Trinkle-Mulcahy L, Lyon CE, Morrice NA, Cohen P, Lamond AI (1997) Purification and characterisation of p99, a nuclear modulator of protein phosphatase 1 activity. FEBS Lett 420(1):57–62

Kruger T, Scheer U (2010) p53 localizes to intranucleolar regions distinct from the ribosome production compartments. J Cell Sci 123(Pt 8):1203–1208. doi:10.1242/jcs.062398

Lachner M, O'Carroll D, Rea S, Mechtler K, Jenuwein T (2001) Methylation of histone H3 lysine 9 creates a binding site for HP1 proteins. Nature 410(6824):116–120. doi:10.1038/3506513235065132

Landsverk HB, Mora-Bermudez F, Landsverk OJ, Hasvold G, Naderi S, Bakke O, Ellenberg J, Collas P, Syljuasen RG, Kuntziger T (2010) The protein phosphatase 1 regulator PNUTS is a new component of the DNA damage response. EMBO Rep 11 (11):868–875. doi:10.1038/embor.2010.134

Latonen L, Moore HM, Bai B, Jaamaa S, Laiho M (2010) Proteasome inhibitors induce nucleolar aggregation of proteasome target proteins and polyadenylated RNA by altering ubiquitin availability. Oncogene. doi:10.1038/onc.2010.469

Legerski RJ (2009) The Pso4 complex splices into the DNA damage response. Cell Cycle 8(21):3448–3449

Linskens MH, Huberman JA (1988) Organization of replication of ribosomal DNA in *Saccharomyces cerevisiae*. Mol Cell Biol 8 (11):4927–4935

Long BH, Musial ST, Brattain MG (1985) Single- and double-strand DNA breakage and repair in human lung adenocarcinoma cells exposed to etoposide and teniposide. Cancer Res 45(7):3106–3112

Loscher M, Fortschegger K, Ritter G, Wostry M, Voglauer R, Schmid JA, Watters S, Rivett AJ, Ajuh P, Lamond AI, Katinger H, Grillari J (2005) Interaction of U-box E3 ligase SNEV with PSMB4, the

beta7 subunit of the 20 S proteasome. Biochem J 388(Pt 2):593–603
Lu X, Legerski RJ (2007) The Prp19/Pso4 core complex undergoes ubiquitylation and structural alterations in response to DNA damage. Biochem Biophys Res Commun 354(4):968–974. doi:10.1016/j.bbrc.2007.01.097
Lundin C, Erixon K, Arnaudeau C, Schultz N, Jenssen D, Meuth M, Helleday T (2002) Different roles for nonhomologous end joining and homologous recombination following replication arrest in mammalian cells. Mol Cell Biol 22(16):5869–5878
Lyon CE, Bohmann K, Sleeman J, Lamond AI (1997) Inhibition of protein dephosphorylation results in the accumulation of splicing snRNPs and coiled bodies within the nucleolus. Exp Cell Res 230(1):84–93. doi:10.1006/excr.1996.3380
Mahajan KN, Mitchell BS (2003) Role of human Pso4 in mammalian DNA repair and association with terminal deoxynucleotidyl transferase. Proc Natl Acad Sci USA 100(19):10746–10751. doi:10.1073/pnas.1631060100
Mahaney BL, Meek K, Lees-Miller SP (2009) Repair of ionizing radiation-induced DNA double-strand breaks by non-homologous end-joining. Biochem J 417(3):639–650. doi:10.1042/BJ20080413
Maiorano D, Lutzmann M, Mechali M (2006) MCM proteins and DNA replication. Curr Opin Cell Biol 18(2):130–136
Mais C, Wright JE, Prieto JL, Raggett SL, McStay B (2005) UBF-binding site arrays form pseudo-NORs and sequester the RNA polymerase I transcription machinery. Genes Dev 19(1):50–64. doi:10.1101/gad.310705
Malatesta M, Zancanaro C, Martin TE, Chan EK, Amalric F, Luhrmann R, Vogel P, Fakan S (1994) Is the coiled body involved in nucleolar functions? Exp Cell Res 211(2):415–419. doi:10.1006/excr.1994.1106
Malatesta M, Gazzanelli G, Battistelli S, Martin TE, Amalric F, Fakan S (2000) Nucleoli undergo structural and molecular modifications during hibernation. Chromosoma 109(7):506–513
Manuelidis L (1984) Different central nervous system cell types display distinct and nonrandom arrangements of satellite DNA sequences. Proc Natl Acad Sci USA 81(10):3123–3127
Manuelidis L, Borden J (1988) Reproducible compartmentalization of individual chromosome domains in human CNS cells revealed by in situ hybridization and three-dimensional reconstruction. Chromosoma 96(6):397–410
Mao I, Liu J, Li X, Luo H (2008) REGgamma, a proteasome activator and beyond? Cell Mol Life Sci 65(24):3971–3980
McStay B, Grummt I (2008) The epigenetics of rRNA genes: from molecular to chromosome biology. Annu Rev Cell Dev Biol 24:131–157. doi:10.1146/annurev.cellbio.24.110707.175259
Meulmeester E, Melchior F (2008) Cell biology: SUMO. Nature 452 (7188):709–711. doi:10.1038/452709a
Moldovan GL, Pfander B, Jentsch S (2007) PCNA, the maestro of the replication fork. Cell 129(4):665–679. doi:10.1016/j.cell.2007.05.003
Murray MV, Kobayashi R, Krainer AR (1999) The type 2 C Ser/Thr phosphatase PP2Cgamma is a pre-mRNA splicing factor. Genes Dev 13(1):87–97
Nakayama J, Rice JC, Strahl BD, Allis CD, Grewal SI (2001) Role of histone H3 lysine 9 methylation in epigenetic control of heterochromatin assembly. Science (New York, NY) 292 (5514):110–113. doi:10.1126/science.10601181060118
Nemeth A, Conesa A, Santoyo-Lopez J, Medina I, Montaner D, Peterfia B, Solovei I, Cremer T, Dopazo J, Langst G (2010) Initial genomics of the human nucleolus. PLoS Genet 6(3): e1000889. doi:10.1371/journal.pgen.1000889
Ochs RL, Press RI (1992) Centromere autoantigens are associated with the nucleolus. Exp Cell Res 200(2):339–350
Ochs RL, Stein TW Jr, Tan EM (1994) Coiled bodies in the nucleolus of breast cancer cells. J Cell Sci 107(Pt 2):385–399
Ogg SC, Lamond AI (2002) Cajal bodies and coilin–moving towards function. J Cell Biol 159(1):17–21
Paredes S, Maggert KA (2009) Ribosomal DNA contributes to global chromatin regulation. Proc Natl Acad Sci USA 106(42):17829–17834. doi:10.1073/pnas.0906811106
Pederson T (1998) The plurifunctional nucleolus. Nucleic Acids Res 26(17):3871–3876
Pederson T, Tsai RY (2009) In search of nonribosomal nucleolar protein function and regulation. J Cell Biol 184(6):771–776. doi:10.1083/jcb.200812014
Peng JC, Karpen GH (2007) H3K9 methylation and RNA interference regulate nucleolar organization and repeated DNA stability. Nat Cell Biol 9(1):25–35. doi:10.1038/ncb1514
Pestov DG, Lapik YR, Lau LF (2008) Assays for ribosomal RNA processing and ribosome assembly. Curr Protoc Cell Biol Chapter 22:Unit 22.11. doi:10.1002/0471143030.cb2211s39
Petri S, Grimmler M, Over S, Fischer U, Gruss OJ (2007) Dephosphorylation of survival motor neurons (SMN) by PPM1G/PP2Cgamma governs Cajal body localization and stability of the SMN complex. J Cell Biol 179(3):451–465. doi:10.1083/jcb.200704163
Potashkin JA, Derby RJ, Spector DL (1990) Differential distribution of factors involved in pre-mRNA processing in the yeast cell nucleus. Mol Cell Biol 10(7):3524–3534
Prokopowich CD, Gregory TR, Crease TJ (2003) The correlation between rDNA copy number and genome size in eukaryotes. Genome 46(1):48–50. doi:10.1139/g02-103g02-103
Rappsilber J, Ryder U, Lamond AI, Mann M (2002) Large-scale proteomic analysis of the human spliceosome. Genome Res 12 (8):1231–1245
Rebelo L, Almeida F, Ramos C, Bohmann K, Lamond AI, Carmo-Fonseca M (1996) The dynamics of coiled bodies in the nucleus of adenovirus-infected cells. Mol Biol Cell 7(7):1137–1151
Ryan AJ, Squires S, Strutt HL, Johnson RT (1991) Camptothecin cytotoxicity in mammalian cells is associated with the induction of persistent double strand breaks in replicating DNA. Nucleic Acids Res 19(12):3295–3300
Sanij E, Hannan RD (2009) The role of UBF in regulating the structure and dynamics of transcriptionally active rDNA chromatin. Epigenetics 4(6):374–382
Santoro R, Grummt I (2005) Epigenetic mechanism of rRNA gene silencing: temporal order of NoRC-mediated histone modification, chromatin remodeling, and DNA methylation. Mol Cell Biol 25 (7):2539–2546. doi:10.1128/MCB.25.7.2539-2546.2005
Santoro R, Li J, Grummt I (2002) The nucleolar remodeling complex NoRC mediates heterochromatin formation and silencing of ribosomal gene transcription. Nat Genet 32(3):393–396. doi:10.1038/ng1010ng1010
Schmitz KM, Mayer C, Postepska A, Grummt I (2010) Interaction of noncoding RNA with the rDNA promoter mediates recruitment of DNMT3b and silencing of rRNA genes. Genes Dev 24 (20):2264–2269. doi:10.1101/gad.590910
Schotta G, Lachner M, Sarma K, Ebert A, Sengupta R, Reuter G, Reinberg D, Jenuwein T (2004) A silencing pathway to induce H3-K9 and H4-K20 trimethylation at constitutive heterochromatin. Genes Dev 18(11):1251–1262. doi:10.1101/gad.300704300704
Shav-Tal Y, Blechman J, Darzacq X, Montagna C, Dye BT, Patton JG, Singer RH, Zipori D (2005) Dynamic sorting of nuclear components into distinct nucleolar caps during transcriptional inhibition. Mol Biol Cell 16(5):2395–2413. doi:10.1091/mbc.E04-11-0992
Shogren-Knaak M, Peterson CL (2006) Switching on chromatin: mechanistic role of histone H4-K16 acetylation. Cell Cycle 5 (13):1361–1365
Sirri V, Urcuqui-Inchima S, Roussel P, Hernandez-Verdun D (2008) Nucleolus: the fascinating nuclear body. Histochem Cell Biol 129 (1):13–31. doi:10.1007/s00418-007-0359-6

Sleeman J (2007) A regulatory role for CRM1 in the multi-directional trafficking of splicing snRNPs in the mammalian nucleus. J Cell Sci 120(Pt 9):1540–1550. doi:10.1242/jcs.001529

Sleeman JE, Lamond AI (1999) Newly assembled snRNPs associate with coiled bodies before speckles, suggesting a nuclear snRNP maturation pathway. Curr Biol 9(19):1065–1074

Sleeman J, Lyon CE, Platani M, Kreivi JP, Lamond AI (1998) Dynamic interactions between splicing snRNPs, coiled bodies and nucleoli revealed using snRNP protein fusions to the green fluorescent protein. Exp Cell Res 243(2):290–304. doi:10.1006/excr.1998.4135

Strohner R, Nemeth A, Jansa P, Hofmann-Rohrer U, Santoro R, Langst G, Grummt I (2001) NoRC—a novel member of mammalian ISWI-containing chromatin remodeling machines. EMBO J 20(17):4892–4900. doi:10.1093/emboj/20.17.4892

Stucki M, Stagljar I, Jonsson ZO, Hubscher U (2001) A coordinated interplay: proteins with multiple functions in DNA replication, DNA repair, cell cycle/checkpoint control, and transcription. Prog Nucleic Acid Res Mol Biol 65:261–298

Tanooka H, Tada M (1975) Reparable lethal DNA damage produced by enzyme-activated 4-hydroxyaminoquinoline 1-oxide. Chem Biol Interact 10(1):11–18

Tornaletti S, Pfeifer GP (1996) UV damage and repair mechanisms in mammalian cells. Bioessays 18(3):221–228. doi:10.1002/bies.950180309

Travis SM, Welsh MJ (1997) PP2C gamma: a human protein phosphatase with a unique acidic domain. FEBS Lett 412(3):415–419

Trinkle-Mulcahy L, Chusainow J, Lam YW, Swift S, Lamond A (2007) Visualization of intracellular PP1 targeting through transiently and stably expressed fluorescent protein fusions. Meth Mol biol (Clifton, NJ) 365:133–154. doi:10.1385/1-59745-267-X:133

Tsai RY, McKay RD (2005) A multistep, GTP-driven mechanism controlling the dynamic cycling of nucleostemin. J Cell Biol 168 (2):179–184. doi:10.1083/jcb.200409053

Tycowski KT, You ZH, Graham PJ, Steitz JA (1998) Modification of U6 spliceosomal RNA is guided by other small RNAs. Mol Cell 2(5):629–638

Ulrich HD (2009) The SUMO system: an overview. Methods Mol Biol (Clifton, NJ 497:3–16. doi:10.1007/978-1-59745-566-4_1

Urrutia R (2003) KRAB-containing zinc-finger repressor proteins. Genome Biol 4(10):231. doi:10.1186/gb-2003-4-10-231

Vakoc CR, Sachdeva MM, Wang H, Blobel GA (2006) Profile of histone lysine methylation across transcribed mammalian chromatin. Mol Cell Biol 26(24):9185–9195. doi:10.1128/MCB.01529-06

van Koningsbruggen S, Gierlinski M, Schofield P, Martin D, Barton GJ, Ariyurek Y, den Dunnen JT, Lamond AI (2010) High-resolution whole-genome sequencing reveals specific chromatin domains from most human chromosomes associate with nucleoli. Mol Biol Cell. doi:10.1091/mbc.E10-06-0508

Westman BJ, Verheggen C, Hutten S, Lam YW, Bertrand E, Lamond AI (2010) A proteomic screen for nucleolar SUMO targets shows SUMOylation modulates the function of Nop5/Nop58. Mol Cell 39(4):618–631. doi:10.1016/j.molcel.2010.07.025

Weterings E, Chen DJ (2007) DNA-dependent protein kinase in nonhomologous end joining: a lock with multiple keys? J Cell Biol 179(2):183–186. doi:10.1083/jcb.200705106

Zannini L, Buscemi G, Fontanella E, Lisanti S, Delia D (2009) REGgamma/PA28gamma proteasome activator interacts with PML and Chk2 and affects PML nuclear bodies number. Cell Cycle 8(15):2399–2407

Zannini L, Lecis D, Buscemi G, Carlessi L, Gasparini P, Fontanella E, Lisanti S, Barton L, Delia D (2008) REGgamma proteasome activator is involved in the maintenance of chromosomal stability. Cell Cycle 7(4):504–512

Zhang N, Kaur R, Lu X, Shen X, Li L, Legerski RJ (2005) The Pso4 mRNA splicing and DNA repair complex interacts with WRN for processing of DNA interstrand cross-links. J Biol Chem 280 (49):40559–40567. doi:10.1074/jbc.M508453200

Zhang N, Kaur R, Akhter S, Legerski RJ (2009) Cdc5L interacts with ATR and is required for the S-phase cell-cycle checkpoint. EMBO Rep 10(9):1029–1035. doi:10.1038/embor.2009.122

Zhou Y, Santoro R, Grummt I (2002) The chromatin remodeling complex NoRC targets HDAC1 to the ribosomal gene promoter and represses RNA polymerase I transcription. EMBO J 21(17):4632–4640

Zuo P, Manley JL (1993) Functional domains of the human splicing factor ASF/SF2. EMBO J 12(12):4727–4737